The Semiannual Cycle of Sea Surface and Free Air Temperatures

by

Wenjie Hu

B.S., Meteorology
Peking University, China
(1990)

Submitted to the Department of Earth, Atmosphere and Planetary Sciences
in partial fulfillment of the requirements for the degree of

Master of Science

at the

MASSACHUSETTS INSTITUTE OF TECHNOLOGY

June 1995

Signature of Author .....
Department of Earth, Atmosphere and Planetary Sciences
April 30, 1995

Certified by .....
Reginald E. Newell
Professor of Meteorology
Thesis Supervisor

Accepted by .....
Thomas H. Jordan
Department Head

The Semiannual Cycle of Sea Surface and Free Air Temperatures

by

Wenjie Hu

Submitted to the Department of Earth, Atmosphere and Planetary Sciences
on April 30, 1995, in partial fulfillment of the
requirements for the degree of
Master of Science

Abstract

Harmonic analysis has been performed on the dataset of the past decade to study the semiannual, annual and interannual variations of free air temperature (measured by satellites with microwave sounding units (MSU)) and sea surface temperature (SST). The results show that in the tropical region the semiannual harmonics of MSU, SST and sea surface solar radiative flux have the maximum contribution to the percentage of total variance. The phase of the semiannual oceanic surface solar radiative flux in the tropic reaches its maximum in March/September while semiannual MSU and SST harmonics get the phase of maximum in May/November. It is proposed that the heating at the sea surface could be the driving force for the semiannual variation of free air temperature of the tropical strip. But currently the data quality of the sea surface latent flux is not good enough to prove such a proposition. Annual harmonics are dominant in the middle and high latitudes but show an asymmetric structure in the tropics, which indicates the atmospheric interactions between the Northern and Southern Hemisphere. The interannual harmonics of MSU and SST mainly reflect the El Niño and Southern Oscillation phenomena, in which MSU data shows the increase of free air temperature in the whole tropical strip when SST rises in the equatorial eastern Pacific.

Thesis Supervisor: Reginald E. Newell
Title: Professor of Meteorology

Acknowledgments

I want to express my gratitude to my advisor, Professor Reginald E. Newell for his invaluable guidance and tremendous encouragement during my study in MIT. His enthusiasm and wonderful physical sense are of great help in my research. I am also indebted to Professors Alan Plumb, Peter Stone, Jochem Marotzke, Kerry Emanuel and Richard Lindzen, for their stimulating teaching and advice, which makes MIT an unusual place to stay.

I would like to express my special thanks to Mr. Wu, Zhongxiang, who kindly provided me the data of the oceanic surface energy flux and offered his helps on many aspects. I also own my gratefulness to Jane MacNubb, Tracy Stanelun, Debra Cochrane and Susan Midlanrsky for their warm-hearted help with the administration. In addition, I want to thanks my wonderful friends Kyle Kapuscinski, Deborah Becker Haarsma, Xiaoli Wang, Xiaomeng Yu and Xiaowei Lu. Their friendship brought me great happiness in the past years.

Finally, I wish to express my appreciation to my parents, for their love and continuing support afar.

This work was supported by the National Science Foundation Climate Dynamics Program under Grant No. ATM-9106902.

Contents

List of Figures

List of Tables

Chapter 1

Introduction

1.1 Motivation

Annual and semiannual cycles are the dominant fluctuations in the seasonal variations of the earth's climate system. The yearly variation of the atmosphere has been well analyzed and better interpreted than the half-yearly one. As is well known, the seasonal change in the distribution of the solar radiation at the top of the atmosphere plays the leading role in the external forcing of the earth's climate, and is responsible for the direct driving for the annual and semiannual cycles. But the direct forcing from the solar radiation is always complicated by the internal processes of the climate system – the feedback effects between the atmosphere, ocean and cryosphere. It's still unclear and hard to estimate how the internal forcing, such as the interaction between ocean and atmosphere, contributes to the periodic cycle of the climate system. Furthermore, the interannual and non-periodic fluctuations also interact nonlinearly with the seasonal periodic cycles. For example, many researchers pointed out that the El Niño and Southern Oscillation (ENSO) phenomena are actually phase-locked with the annual cycles (Rasmusson and Carpenter 1982; Meehl 1987).

To study seasonal and long-term atmospheric variations, the oceanic influence must be taken into account. The oceanic energy flux (latent and sensible heat flux) plays an important role in balancing the atmospheric energy budget. The correlation between the seasonal and nonseasonal variations of the atmospheric free air tempera-

ture, sea surface temperature (SST) and oceanic surface heat flux has been analyzed through regular empirical orthogonal function (EOF) methods by Hu, Newell and Wu (1994) (it is referenced as the mode paper in the present thesis). Their results show that the annual and semiannual cycles are dominant in the seasonal EOF modes while the ENSO phenomena are the largest signal in the nonseasonal modes of free air temperature, SST and surface solar heat flux. The heat flux from the ocean surface leads to the amplitude reduction and phase lag of the annual cycle of the free air temperature over oceanic areas. In addition, the increase of latent heat flux due to the positive SST anomalies in the equatorial oceanic Pacific is responsible for the warmth of the atmospheric temperature in the whole tropical strip. But it is unclear how the semiannual cycle of the free air and oceanic surface temperature are linked to each other. In the eigenvector analysis, the data field is split into spatial and temporal parts. Only the dominant patterns are considered in the EOF analysis. But EOF methods may not distinguish completely the variabilities at certain periodic time scales. For example, in the second EOF seasonal mode of free air temperature (Hu, Newell and Wu, 1994), both nonseasonal El Niño modes and semiannual cycles are involved. In the present paper, harmonic analysis, which is good at getting the phase and amplitude of the pure sinusoidal cycles, is applied to study the periodic variations of the atmosphere. Some comparisons will be made between the two methods.

The feedback process from the atmosphere always complicates the variations of oceanic and atmospheric temperature. Corresponding to the SST enhancement, the distribution of clouds and water vapor content in the atmosphere, as well as the atmospheric circulation, would change. The radiative change caused by clouds and atmospheric water vapor content could lead to significant change on both oceanic and free air temperature. But such effects are hard to estimate due to the difficulties in the measurement of cloud and atmosphere water vapor, which are closely related to atmospheric convection with an hour-long time scale. Currently, it is still unclear how much the feedback effect would be on the air temperature following the forcing of the surface oceanic boundary. Thus, analyzing the patterns of the periodical variations at yearly and half-yearly time scales, in addition to the interannual oscillations, would

be helpful in understanding the mechanisms of the interaction between air and sea.

1.2 Background study

The study of climate fluctuations from time scales of months to decades has been expanded in the past two decades with the fast growth of global data coverage and development of general circulation models (GCMs). Both seasonal and nonseasonal (interannual) variations have been studied. Since the large thermal capacity of the ocean provides a long term memory of the climate change, the interaction between ocean and atmosphere has become one of the important issues in the climate study.

1.2.1 Seasonal variations

Different from the symmetric solar forcing at the top of the atmosphere, the seasonal varations in the atmosphere always show asymmetries with latitudes (Van Loon and Jenne 1969; Van Loon and Jenne 1970; Hsu and Wallace 1976a and 1976b). Before the availability of long-term global data, the observational studies of climate variability of the atmosphere were mainly limited to the radiosonde data at stations which are mostly over the land while large remote oceanic areas are not covered. The studies on the annual and semiannual cycles indicated that large semiannual variations are found in the tropical and high-latitude polar regions. They are associated with the astronomical cycle of the direct solar radiation. After calculating the harmonics of the atmospheric wind and temperature at 60°E-120°E, Van Loon and Jenne (1970) proposed that the north-south movement of the upward branches of Hadley cells causes the half-yearly fluctuations of the tropical atmospheric temperature.

With the development of GCMs and growth of atmospheric data coverage, the decade long global-coverage data became available, such as real time European Center Medium-Range Weather Forecasts (ECMWF) and National Meteorological Center (NMC) grid-point products. The improvement of data coverage gave impetus to the climate study on seasonal and interannual fluctations. Weichman and Chervin (1988) compared long term NMC wind data with the results simulated by atmospheric GCM.

Their results showed that the atmospheric GCM captured well the features of annual cycles but there are large discrepencies in the semiannual cycles. They also suggested that an east-west circulation could exist in the tropics associated with the semiannual cycle of clouds. Following Weichman and Chervin's hypothesis, Chen and Wu (1992) derived the wave number one patterns after calculating the semiannual cycle of the velocity potential and out-going longwave radiation (OLR) in the tropics. The corresponding phase of the maximum of the semiannual cycle is in April/October. They pointed out that the differential heating between the Asian-Australian (AA) monsoon hemisphere (60°E-120°W, ocean dominant) and extra-AA monsoon hemisphere (120°W-60°E, land dominant) induces the east-west circulation in the tropics. It suggests that apart from direct solar forcing, the thermal forcing from the underlying surface also drives the semiannual cycle of atmospheric circulation.

The asymmetric structure of the annual and semiannual cycles are also shown in the seasonal EOF analysis (Hu, Newell and Wu, 1994). The first, second and third seasonal EOF patterns for SST and oceanic surface solar flux, which show annual and semiannual cycles in the time series, all have zonally asymmetric structures in the tropics. The correlation calculation indicates that the annual variation of the air temperature over ocean is one month lagged on the one over land. Obviously, to interpret the atmospheric asymmetries, different surface forcing needs to be considered.

1.2.2 Nonseasonal variations

ENSO is one of the phenomena of most concern in the climate study of past two decades. Its process has been well described by Rasmusson and Carpenter (1982) and Deser and Wallace (1990). In term of the ENSO physical mechanisms, Bjerknes (1969) proposed that the evaporative anomalies caused by the increase of SST in the tropical east Pacific are the driving force on the shift of Walker circulation in the tropics as well as the global climate variations. Based on Bjerknes's hypothesis, the sources and sinks of the energy in the model simulations are specified or parameterized as a function of SST anomalies or SST itself (Webster 1972,1978; Gill 1980; Lau 1985). General states of the El Niño phenomena have been produced by the model successfully, but

detailed comparison between models and observations are not plentiful due to the insufficient simulation and the complexity of climate system (Barnett, et. al. 1991).

Many researchers have already shown the good correlations between the atmospheric temperature in the tropics and SST in the equatorial eastern Pacific (Pan and Oort 1983; Newell and Wu 1992). The increase of surface evaporation in the coastal region of tropical eastern Pacific was proposed to explain the enhancement of air temperature in the whole tropical strip (Hu, Newell and Wu 1994). The downward motions of Walker cell are responsible for the temperature increase of the tropical zone (Wu 1994, personal communication).

1.2.3 Atmospheric feedback processes

Atmospheric feedback processes on the oceanic heating source always causes the complexity of the climate fluctuations. Ramanathan and Collins (1989) studied the cloud forcing from the Earth Radiation Budget Experiement and concluded that the size of the observed cloud net cooling is about four times as large as the expected radiative cooling from a doubling of CO_2. Thus, a small change in the cloud-radiative forcing can play a significant role as a climate feedback mechanism. Then associated with ENSO phenomena, Ramanathan and Collins (1992) suggested that the upper-level cirrus cloud from deep convection prevents the increase of SST. However, Fu, Rossow and Del Genio (1992) argues that oceanic surface latent heat flux plays the main role in buffering the increase of SST. Wallace (1992) also questioned about Ramanathan and Collins's hypothesis and emphasized the importance of large-scale circulations on the control of SST upper limits. In the mode paper, both radiative and ocean surface evaporative cooling effects are important on the feedback of SST heating.

1.3 Goal and organization of the thesis

In the current thesis, the method of harmonics analysis is applied to the grid-by-grid dataset. The decadal free air temperature, SST and surface oceanic flux data are analyzed at both seasonal and nonseasonal time scales. It is attempted to find out

the driving factors on the variations of free air temperature and estimate the oceanic effects on the change of atmospheric temperature.

The structure of the thesis will be organized as follows. Motivation and background study have been addressed in current chapter. Data sources and analysis procedures will be given in chapter two. The amplitudes and phases for semiannual, annual and interannual variations are going to be presented in chapter three. The discussion is concentrated in chapter four with a focus on semiannual cycle. Chapter five is the summary and suggestions of future work.

Chapter 2

Data Sources and Analysis Approaches

2.1 Data sources

The free air and sea surface temperature data , as well as oceanic surface energy flux, which is the linkage between air and sea surface temperature fields, will be used in this thesis for calculations.

The data set of the tropospheric free air temperature is from the TIROS-N satellite series Microwave Sounding Unit (MSU), which is channel 2 brightness temperature during 1979-1992, with monthly 2.5° by 2.5° gridpoints. MSU channel 2 measurements are dominated by vertically weighted air temperature through a deep tropospheric layer. Its weighting function has a broad vertical distribution from the surface to above 30kPa(see Figure 2.1) with peak between 50-70 kPa(Spencer and Christy 1990). The intercomparisons between radiosonde data and simultaneously operating MSU measurements reveal agreement to 0.01°C for monthly globally averaged anomalies (Spencer and Christy 1990). At the 2.5° gridpoint scale the precision of the satellite measurement also indicates good agreement with radiosonde data on the monthly anomalies, with correlation coefficients from 0.94 to 0.98. MSU dataset shows the characteristics of an integrated structure of free air temperature.

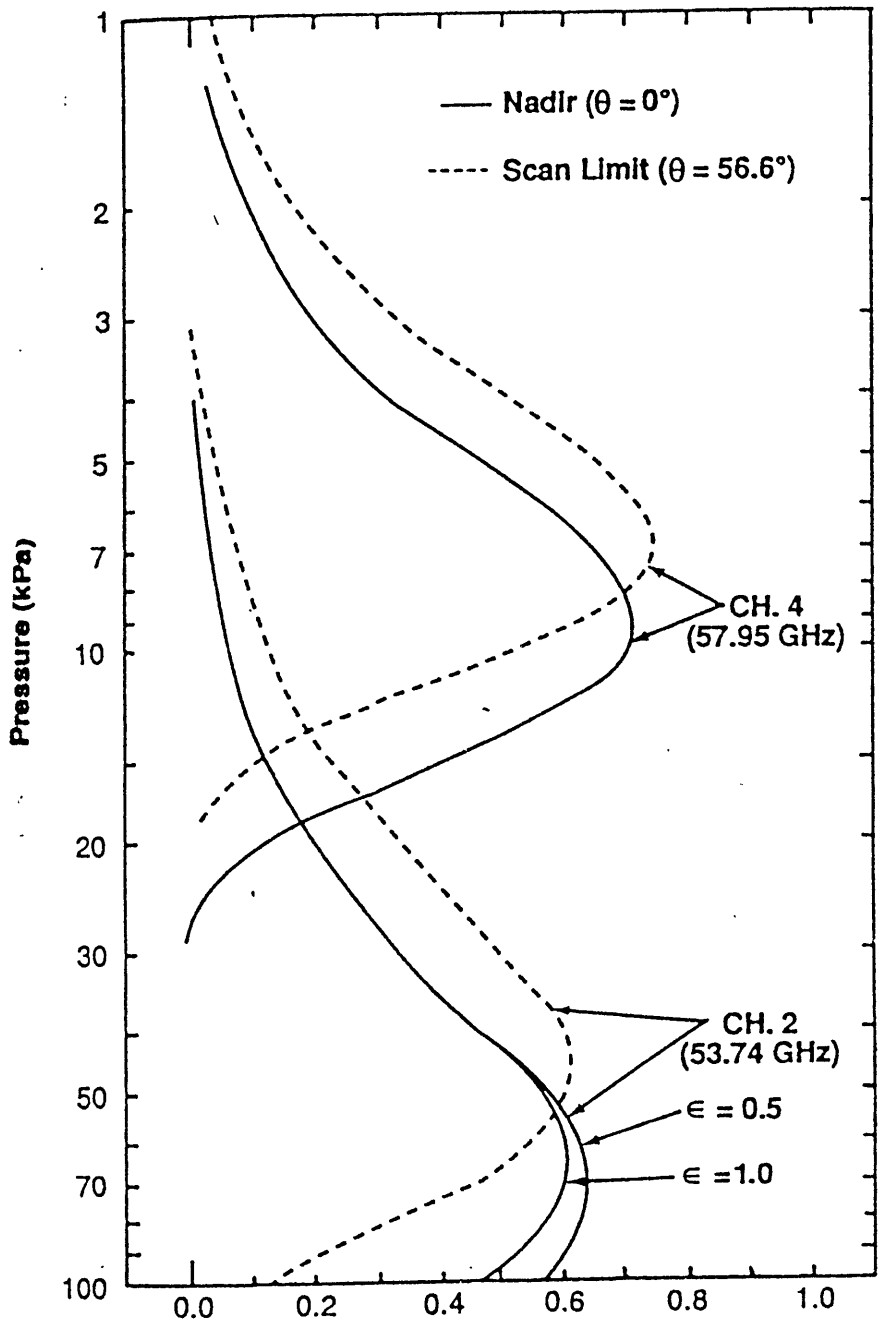

Figure 2-1: Temperature weighting function of MSU data at channel 2 (after Spencer, Christy and Grody 1990).

The oceanic dataset is from Comprehensive Ocean Atmosphere Data Set (COADS) with a resolution of 2° by 2° for global coverage from 1949-1987, including SST, surface wind, air temperature and moisture from the merchant ship measurements. Since the current paper is going to focus on the semiannual cycle in the tropics, only oceanic surface latent heat and solar flux, which both are the large term in the variation of tropical SST budget equation, are used for the analysis (Hsiung 1986). The oceanic surface solar and latent heat flux can be calculated through the bulk formula (Hsiung 1986):

$$Q_{sol} = Q_0 T_r (1 - A)(1 - 0.62c + 0.0019\alpha) \tag{2.1}$$

$$Q_{lat} = \rho_a L C_e V (q_s(T_s) - q_a(T_a)) \tag{2.2}$$

Where Q_{sol} and Q_{lat} represent individually the oceanic surface energy flux of solar radiative and latent heat flux. The meaning of other symbols can be found in Table 2.1. The cloud coefficient is taken from Budyko's atlas (1963), and the transfer coefficient (C_e) for latent heat in the bulk formula was taken from Large and Pond (1982). Instead of using constant coefficients as Bunker(1976) did, Large and Pond revised the coefficient, which increases with wind speed and increases inversely with vertical stability, indicated by the surface air and sea temperature difference. The calculation of oceanic energy flux was done by Mr. Wu Zhongxiang and used to apply the analysis in this thesis.

Because of the uncertainties in the bulk formula and marine observations, the latent heat flux show relatively large error bars. As noted by Weare, Strub and Sauel (1981), Cayan (1992), the only satisfactory way to estimate the latent heat flux is to average over several samples. The random errors would be diminished by averaging over space and time. Thus the long-term mean over large areas of ocean should be more reliable. The non-random data errors, caused by biases in the bulk formula and the change of instruments can not be reduced from averaging the monthly data. But the non-random error bar in the anomaly fields would be partially reduced by removing the monthly mean values. The error bar given by Hsiung (1986) is about

Table 2.1: Definition of symbols in the bulk formula

α	solar noon altitude in degrees
ϵ	emissivity of water taken as 0.97
ρ_a	air density
σ	Stefan-Boltzman constant
A	albedo at sea surface taken from Payne (1972)
b	the cloud coefficient taken from Budyko's atlas (1963)
C_e	transfer coefficient for latent heat of evaporation taken from Large and Pond (1982)
C_p	specific heat of air
c	cloud amount in tenths
e	water vapor pressure
Q_a	specific humidity of the air
Q_s	saturation of specific humidity at T_s
T_a	temperature of the air
T_s	temperature of sea surface
T_r	atmospheric transmissivity
V	wind speed

10% to 20% for the monthly mean latent heat fluxes.

In the tropical ocean, the observational analysis is always bothered by insufficient sampling. To the south of 30°S, there is almost no data. Approximations to the missing data points were obtained by interpolation from the adjacent areas with better data coverage. The observational data has been much improved in the past decade through a series of oceanic and atmospheric experiments in the tropical ocean. The oceanic data were mainly used during period of 1978-1987 to compare with the simultanenous MSU data. In the calculation of the correlation among MSU, SST and sea surface heat flux, each data set was interpolated to 5° by 5° grid points.

2.2 Analysis approaches

The harmonic analysis is performed in the time series of data fields (see Jenkins & Watts 1968). Amplitude and phase representation in the current thesis are defined in this form

$$s(t) = R_0 + 2\sum_{m=1}^{n-1} R_m cos(2\pi mft - \phi_m) + R_n cos(2\pi ft) \tag{2.3}$$

where

$$R_m = \sqrt{A_m^2 + B_m^2}, \qquad \phi_m = arctan(\frac{B_m}{A_m}) \tag{2.4}$$

and

$$A_m = R_m cos(\phi_m), \qquad B_m = R_m sin(\phi_m) \tag{2.5}$$

Here n is one half of total discrete time periods N for certain discrete time series s(t). R_m is the amplitude and ϕ_m the phase of the m harmonic relative to an arbitrary origin time. R_n is the amplitude of the harmonics at one half of total time periods N. $f = 1/(N\delta)$, δ is the minimum sampling period. In the current thesis, all the time series are adjusted to start from January. For all data sets the minimum sampling data is month.

The *variance* is defined as

$$\sigma^2 = 2 \sum_{m=1}^{n-1} R_m^2 + R_n^2 \tag{2.6}$$

The contribution of each harmonic to the total variance can be calculated by $2*R_m^2/\sigma^2$ (for m less than n).

Different from EOF analysis, harmonic analysis provides information on the power and phase of the individual spectrum while EOF methods may mix annual and semi-annual variance resulting from relaxing the requirement for representing the observed data with a pure sinusoid. But eigenvector analysis has the advantage of more precisely defining the dominant patterns with nonsinusoidal oscillation. The requirement for spatial and temporal orthogonality in eigenvector analysis could also cause the differences from the results of harmonic analysis. The comparisons between the two approaches will be given in next chapter.

Chapter 3

Harmonic Analysis of SST, MSU and Oceanic Surface Energy Flux

3.1 Introduction

In the current chapter, the results of harmonic analysis on MSU, SST, Q_{lat} as well as Q_{sol} will be presented at semiannual, annual and interannual time scales. The variations of zonal average will be given at the beginning and then variance in the tropical region will be emphasized. EOF analysis on the same components is presented in Hu, Newell and Wu's (1994) paper, in which annual and semiannual fluctuations are dominant in the seasonal modes and ENSO phenomena are the largest signals in the nonseasonal modes. Restricted by the orthogonal analysis, EOF method is good at choosing the first several dominant patterns instead of picking up particular fluctuations. Different from the eigenvector method, harmonic analysis distinguishes the amplitude and phase of the different harmonics without mixing them. In this chapter, monthly dataset is used for the calculation of harmonic analysis. All time series are set to start in January. And the phase zero is defined as January 16 in the current paper. The results from free air temperature(MSU) and SST data are compared and the oceanic surface energy flux Q_{sol} and Q_{lat} are also investigated in an attempt to find the correlation between the two temperature fields. The discussion will be carried on in the next chapter.

3.2 Latitudinal distributions of annual, semiannual and interannual harmonics

Harmonic analysis was applied on the zonal mean MSU, SST, Q_{sol} and Q_{lat} time series. The total variances of annual, semiannual and interannual (greater than and equal to two years) harmonics are plotted in Figure 3.1. The amplitude and the phase of annual and semiannual harmonics are given in Figure 3.2 and 3.3. Figure 3.4 shows the ratios of semiannual to annual oscillations.

For interannual harmonics, the percentage of total variance is relatively large for SST and air temperature in the tropics (20N-20S). The maximum percentage is about 50% for MSU and 30% for SST. The percentage of total variances contributed by Q_{lat} and Q_{sol} interannual harmonics are quite small for all latitudes, less than 10%. In the middle and high latitudes, the contributions from SST and MSU interannual harmonics have only a few percent.

The zonal distributions of the amplitude of annual harmonics (left column of Figure 3.2) are asymmetric with the hemisphere. The amplitudes of MSU, SST and Q_{lat} in the NH middle latitude are twice as large as the ones in the Southern Hemisphere(SH), which could be associated with larger land masses in the NH. The phase of annual harmonics for each component is also plotted in the right column of Figure 3.2. The time axis is labeled as 1=January 1; 2=February 1. For MSU, SST and Q_{sol}, the phases of maximum for both hemispheres are in summer time while the maximum of annual harmonics in the tropics occurs in the NH spring/autumn time. For Q_{sol}, the phase of the maximum appears in June for NH 20N-70N and December for SH 5S-47.5S. For the free air temperature, the maximum appears in August for NH 20N-90N and February for SH 20S-90S. The date for the maximum SST is about one month lagged on MSU. It is September in NH 15N-70N and March in SH 10S-50S. Q_{lat} has its maximum in winter, which is December in NH 15N-70N and June/July in SH 15S-47.5S.

The amplitude and phase of semiannual harmonics are given in Figure 3.3. In the tropics, the phases of maximum of Q_{sol}, SST and MSU are in the transition seasons

(spring and autumn). But Q_{lat} $(30N - 25S)$ has its maximum in June/December. The maximum of Q_{sol} semiannual harmonics $(25N - 25S)$ appears in March/August; for both MSU $(20N - 15S)$ and SST $(25N - 25S)$, the maximum are at the end of April/September. Although the amplitude of semiannual harmonic may increase with latitudes, the percentage of total variance becomes much smaller in the middle and high latitudes. The phase for the first maximum of semiannual oscillation also varies latitudinally for different components. The maximum is in January/July for MSU in the NH $25N$ to polar region . But in the SH middle and high latitudes, the phase of MSU semiannual harmonic really varies. From $20S$ to about $45S$, MSU has the maximum in February/August. And the phase gradually changes to January/June in the polar region. For SST, the phase of the semiannual maximum is February/August. For Q_{sol}, the phase of the maximum in the middle latitude changes to summer/winter season in the polar region. In the NH middle latitudes, the maximum for Q_{lat} is April/October. But in the SH middle latitude, the phase of the maximum varies from June/December in $20S$ to January/July in $40S$.

The ratios of semiannual to annual amplitudes are shown in Figure 3.4. Values greater than 0.20 are concentrated between 20N and 20S. In the middle and high latitudes, the ratio is so small that the annual oscillations are dominant. The ratios are also equatorial asymmetries. The maximum of the ratios of Q_{sol}, Q_{lat} and SST are to the north of the equator.

3.3 Harmonic analysis results in the tropics

From the above calculations, we can see that semiannual and interannual harmonics all play important parts in shaping the percentage of total variance curve in the tropics. But in the middle and higher latitudes the annual harmonics are dominant. Although the amplitude of semiannual harmonics is relatively large in the high latitudes in contrast to the values in the tropics, its contribution to the total variance is small (such as MSU). In the next sections, the total variance, amplitude and phase of the maximum from semiannual, annual and interannual oscillations are mapped

between 40N-40S. The structure in the tropical area is stressed.

3.3.1 Maps of semiannual harmonics ($40N - 40S$)

Figure 3.5 shows the percentage of total variance as well as the amplitude and phase of the maximum from the MSU semiannual harmonic. The semiannual MSU oscillation represents 15% of total variance in the tropical west Pacific, the tropical Atlantic and the eastern part of South America (Figure 3.5a), but less than 5% in the tropical central Pacific and subtropics. The amplitude of MSU semiannual harmonic (Figure 3.5b) is about $0.1°C$ in the tropics, 20N-20S. In the subtropics the amplitude is larger than that in the tropics but the percentage of total variance is smaller. The phase of the maximum of MSU semiannual harmonics in the tropical central and eastern Pacific (Figure 3.5c) seems to suggest the influence from North America . In the tropics, the phase of MSU first maximum is May in most of the Indian and Pacific Ocean and April in South America, Atlantic and Africa.

The percentage of total variance of SST semiannual oscillation is longitudinally asymmetric. The percentage is 50% in the Northern Indian Ocean and 20% in the tropical west Pacific (Figure 3.6a). In the other areas, the percentage contributed by semiannual harmonics is less than 10%. The amplitude (Figure 3.6b) in the northern Indian monsoon region has its maximum $0.7°C$. In tropical west Pacific and eastern Atlantic the amplitudes are only $0.2 - 0.3°C$. The phase of the maximum of SST semiannual harmonic is in May/June (November/December) in most tropical areas (Figure 3.6c). But the phase of the maximum in the southern eastern Pacific varies a lot, in which the oceanic upwelling is a dominant term in the SST heat budget.

The large contributions of Q_{sol} semiannual oscillations are mainly concentrated in three areas: northern Indian Ocean, tropical west Pacific as well as tropical Atlantic (Figure 3.7a). The total variance is more than 25% in those regions. In the tropical central and eastern Pacific the semiannual harmonic only represents 5% of the total variance . The amplitude of Q_{sol} semiannual harmonic (Figure 3.7b) is greater than 10 W/M2 in the western Pacific and Northern Indian Ocean. The phase of Q_{sol} (Figure 3.7c) has the maximum in March(September) in the tropical Indian Ocean,

central Pacific and Atlantic, and April (October) in the tropical west and east Pacific, northern and southern Indian Ocean.

The percentage of total variance of semiannual Q_{lat} harmoincs (Figure 3.8a) also shows large zonal asymmetry in the tropics, with relatively large contribution in the northern Indian Ocean, tropical monsoon region and tropical eastern Atlantic. The largest amplitude of semiannual Q_{lat} (Figure 3.8b) is in the northern Indian ocean with the maximum phase in January/July, which is not in phase with SST semiannual peaks in May/November. In the other tropical areas, the phase for the first maximum of semiannual Q_{lat} (Figure 3.8c) varies from March to June. Would the variations of semiannual Q_{lat} be caused by the oscillations of oceanic surface wind? The percentage of total variance from semiannual harmonics of oceanic surface wind speed (Figure 3.9a) has the similar pattern as Q_{lat} in the Indian monsoon and tropical west Pacific. The large amplitudes of semiannual harmonics of surface wind speed also show in the same region (Figure 3.9b). But the phase of the first maximum of semiannual surface wind speed (Figure 3.9c) shows large discrepancies with the phase of the maximum of semiannual Q_{lat}, even in the Indian monsoon and topical west Pacific.

3.3.2 Maps of annual harmonics ($40N - 40S$)

The percentage of the variance contributed from the MSU annual harmonic is more zonally symmetric in the tropical and subtropical regions(Figure 3.10a). It varies from 10% to 30% in the equator. It is less than 10% in the tropical central Pacific and eastern South America. It implies that there is less communication on the annual oscillations between NH and SH in those areas. To the north of 20N, the annual harmonic represents above 90% of total variance; and to the south of 20S, MSU annual harmonic represents 40-80% of total variance. The large gradients of total variance from annual harmonics are located in the subtropical region. Generally, the amplitude of MSU annual harmonic is about $0.5°C$ in the tropics (Figure 3.10b). But the amplitude in the tropical west and central Pacific and tropical eastern South America is very small(less than $0.1°C$). In the NH, the amplitude of annual oscillation and its gradients are larger than those in the SH. The phase of annual harmonic

(Figure 3.10c) has no symmetric zonal distribution in the tropics, ranging from March to July. In the tropical central Pacific(180-140W) and South America(70W-40W), where the amplitude of annual harmonic is very small, the phase of the maximum of annual harmoinc has large longitudinual transition from March/April to June/July. Over the tropical west Pacific, the phase of MSU annual harmonic has the maximum in March while over the equatorial Indian Ocean and Atlantic, the annual oscillation shows its maximum in April/May.

For SST, the percentage of total variance from annual harmonic (Figure 3.11a) is relatively zonally symmetric in the tropical oceans. But in the equatorial central Pacific the percentage of total variance reaches smallest value (less than 10%). The amplitude of SST annual harmonic (Figure 3.11b) is about $0.5°C$ in the topics and increases poleward. The phase of SST annual harmonic (Figure 3.11c) shows the maximum SST occurs in September in NH middle latitudes and March in SH middle latitudes. In the tropics the phase of the maximum transits from March in the SH to September in the NH. The phase of SST annual maximum shows equatorial asymmetric, which is close to the SST seasonal EOF #1 mode (Hu, Newell and Wu, 1994).

The percentage of total variance contributed by the Q_{sol} annual harmonic decreases equatorward (Figure 3.12a). Q_{sol} annual harmonic only contributes 10-20% of the total variance in the tropical Pacific and Atlantic. The amplitude of Q_{sol} (Figure 3.12b) shows zonally symmetric distribution. But the phase of the annual harmonic (Figure 3.12c) shows the longitudinally asymmetric structure. In the tropical east Pacific and east Atlantic, the phase of the maximum is in March-May. In the tropical west and central Pacific, the phase of maximum distributes more zonally, varying from November in the SH to July in the NH. In the central Indian Ocean, the dominant phase of the annual Q_{sol} maximum is in March.

The percentage of total variance and the amplitude of Q_{lat} annual harmonic(Figure 3.13a & b) are similiar to the pattern of seasonal EOF #1 in the mode paper(Hu, Newell and Wu, 1994), with large weightings in the west oceanic areas of the middle latitudes. In the tropics, the amplitude is about 4-8 W/M^2. The phase of the max-

imum (Figure 3.13c) is zonally asymmetric in the tropics, varying from February to October. In the NH middle latitudes, the maximum phase in the west Pacific and Atlantic is in December, which is consistent with EOF results. The percentage of total variance and amplitude of the annual surface wind speed (Figure 3.14a,b) have more complex structures than the Q_{lat} patterns in the tropics. The amplitude of the annual harmonics of oceanic surface wind speed has large values in the northern Pacific and Atlantic, and the Indian monsoon regions. The phase of the maximum of oceanic surface wind (Figure 3.14c) is not in phase with the Q_{lat} annual oscillations.

3.3.3 Ratios of semiannual to annual variations (40N–40S)

Though the zonal mean semiannual harmonic of Q_{sol} exceeds the annual harmonic in the tropics, the semiannual harmonics do not dominate everywhere in the equatorial regions. The ratio of semiannual to annual amplitude for each component is plotted in Figure 3.15. For SST, Q_{sol},Q_{lat}, and oceanic surface wind speed, the ratios greater than one are mainly in the tropical west Pacific and northern Indian Ocean (Figure 3.15b,c,d,e). Semiannual MSU oscillations are mainly greater than the annual ones in the three areas: tropical west Pacific, tropical central Pacific and eastern South America (Figure 3.15a). As is shown in the last section, the MSU annual oscillations have very small contributions in the tropical central Pacific and eastern South America.

3.3.4 Interannual harmonics (40n–40S)

The percentage of total variance of the interannual oscillations (greater than two years) for each component is shown in Figure 3.16. The largest values are mainly concentrated in the tropical Pacific. The MSU interannual harmonic (Figure 3.16a) contributes more than 10% of total variance in the tropical belt, with the maximum greater than 50% in the tropical middle and east Pacific. The interannual SST harmonics (Figure 3.15b) contributes about 20% of total variance in the middle and east Pacific. But there is about 10% in the tropical Indian and west Pacific ocean. The

interannual harmonics of Q_{sol} represents about 10% of total variance in the tropical west and central Pacific but less than 10% in the other tropical regions(Figure 3.16c). For Q_{lat} (Figure 3.16d), the largest percentage of total variance from interannual harmonics is 10% in the tropical east Pacific. The contribution from interannual harmonics of oceanic surface wind speed is larger than 10% in the tropical middle and east Pacific.

In the mode paper by Hu, Newell and Wu(1994) the results show that Q_{lat} and SST are well coupled with MSU varaitions in the tropical east Pacific but not in the west Pacific. It seems that the evaporation in the small region of tropical east Pacific causes the change of the air temperature in the entire tropical strip. There is no direct surface latent heat linkage between free air temperature and SST in the other areas.

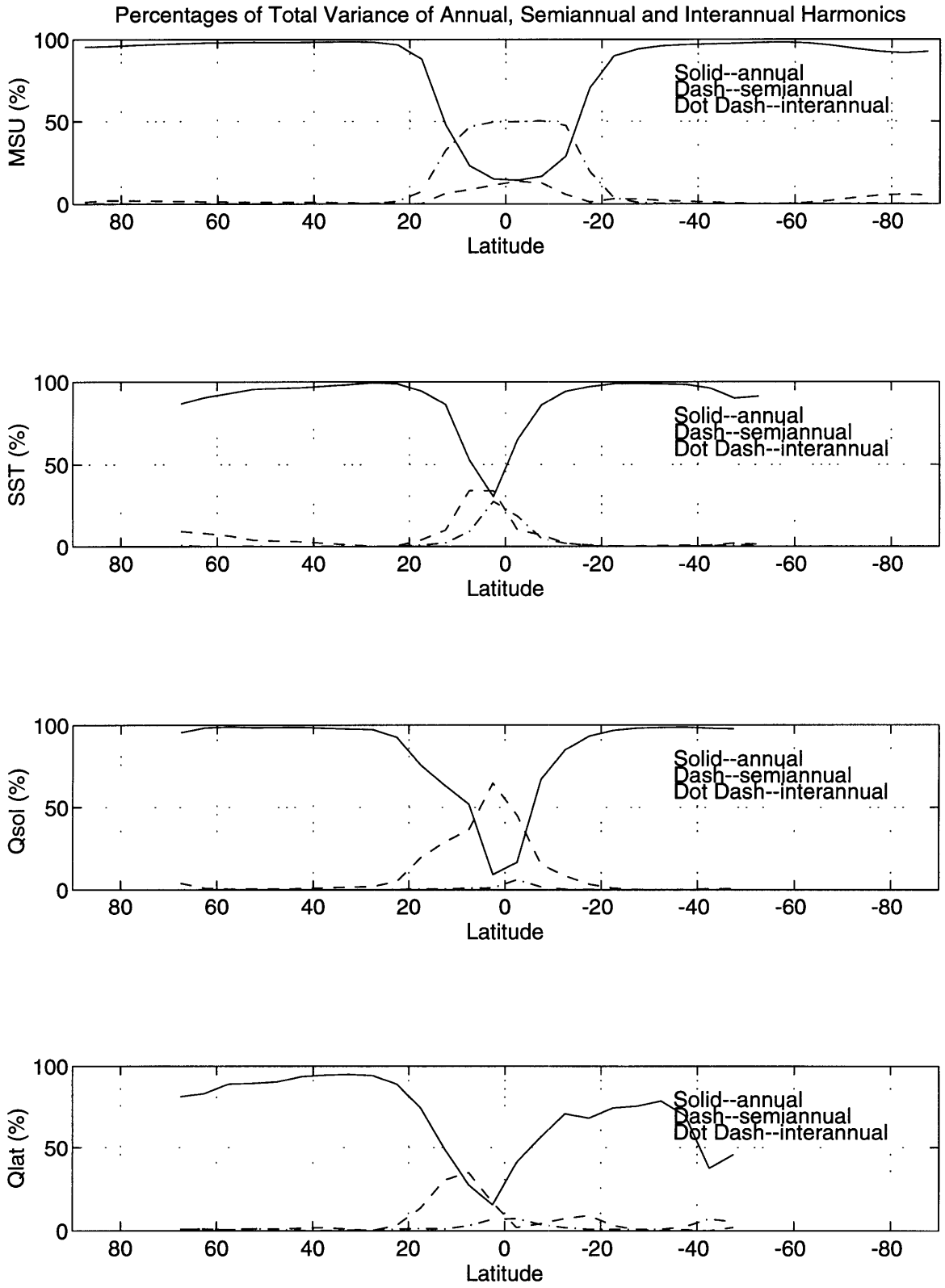

Figure 3-1: Percentage of total variance for annual, semiannual and interannual harmonics of zonally averaged MSU, SST, Q_{sol} and $Qlat$.

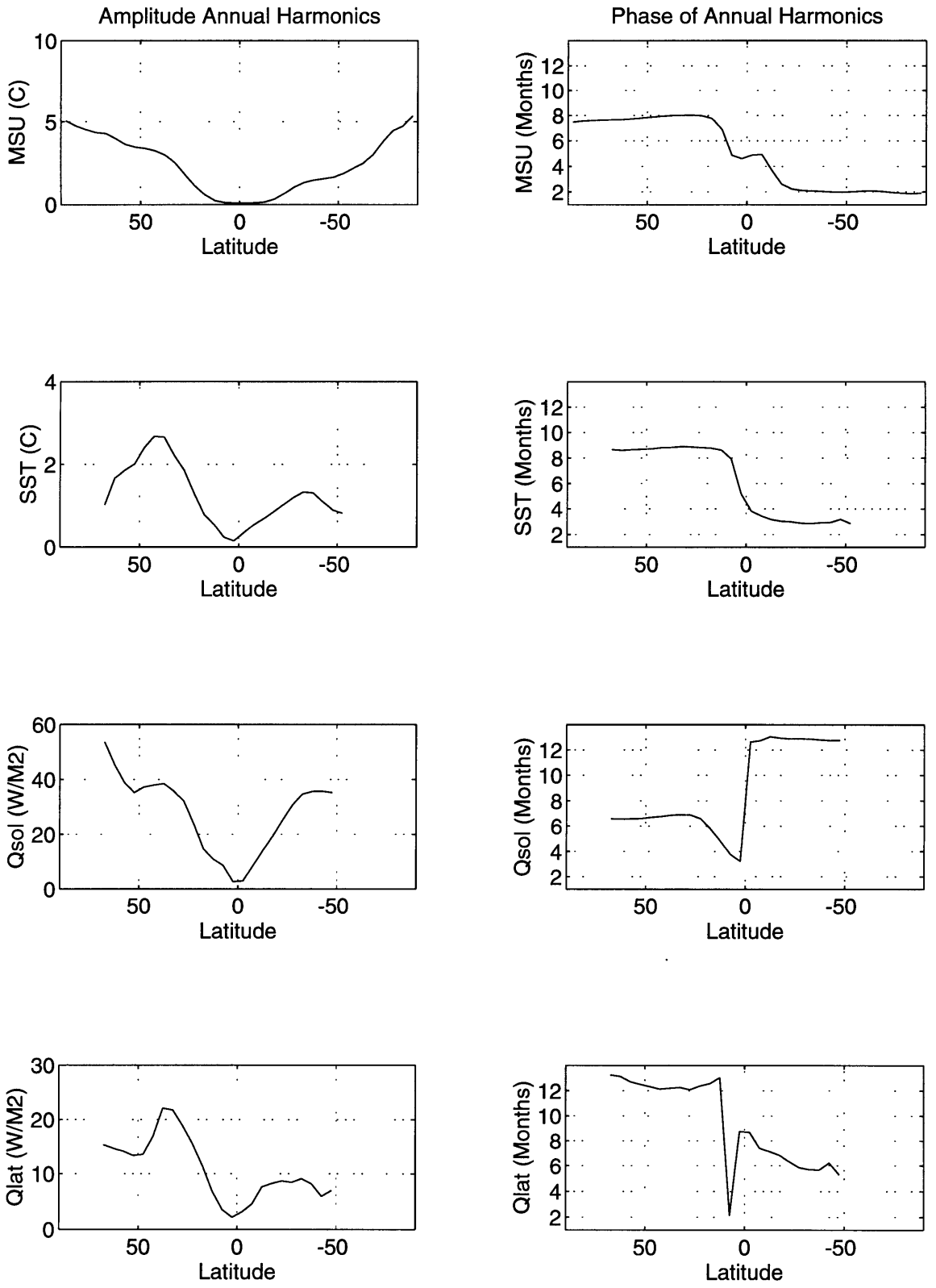

Figure 3-2: Amplitudes and phases of zonal averaged annual harmonics of MSU, SST, Q_{sol} and Q_{lat}.The phase is marked as 1=January 1; 2=February1.

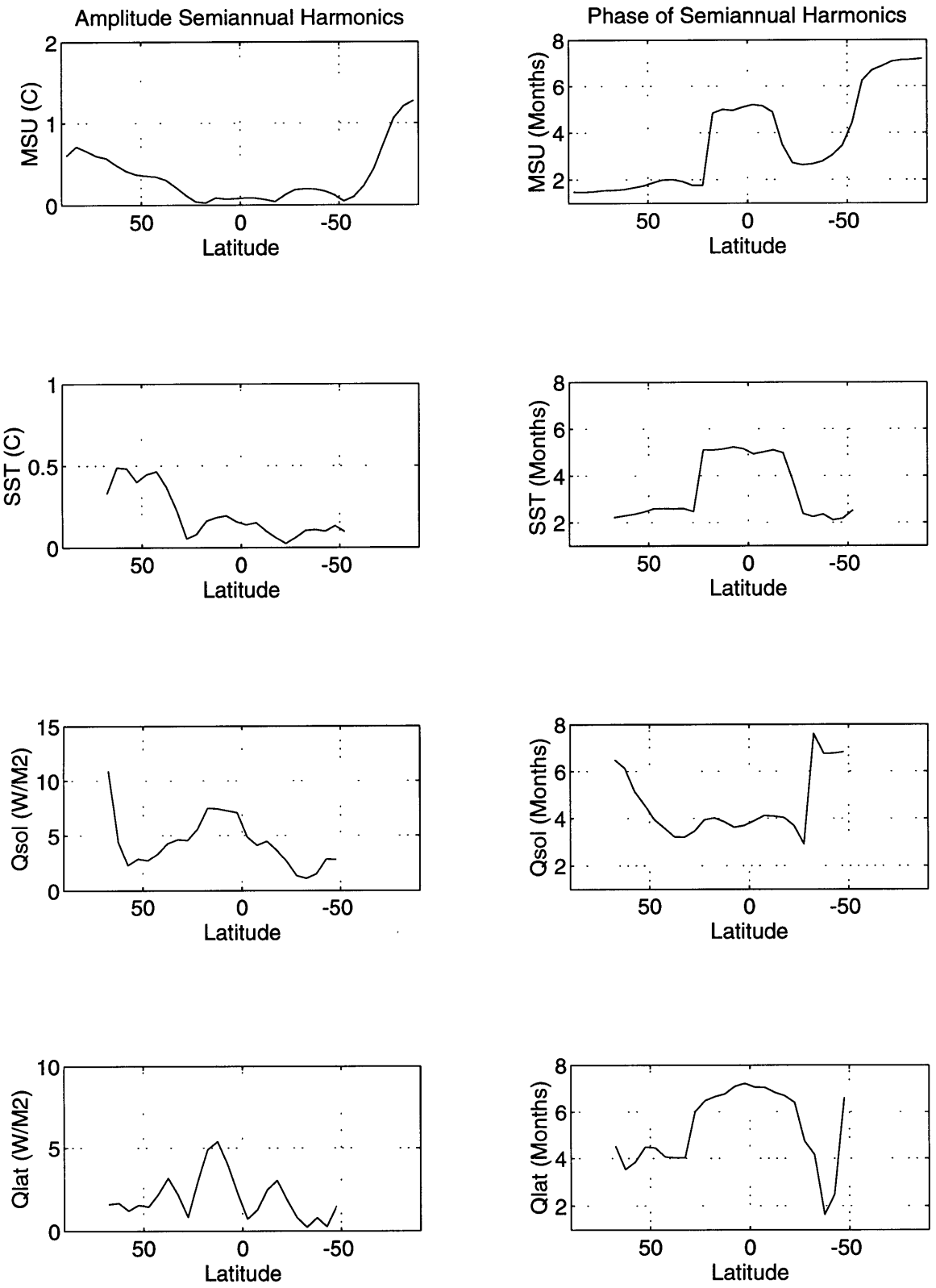

Figure 3-3: Amplitudes and phases of zonal averaged semiannual harmonics of MSU, SST, Q_{sol} and Q_{lat}. The phase is marked as 1=January 1; 2=February 1.

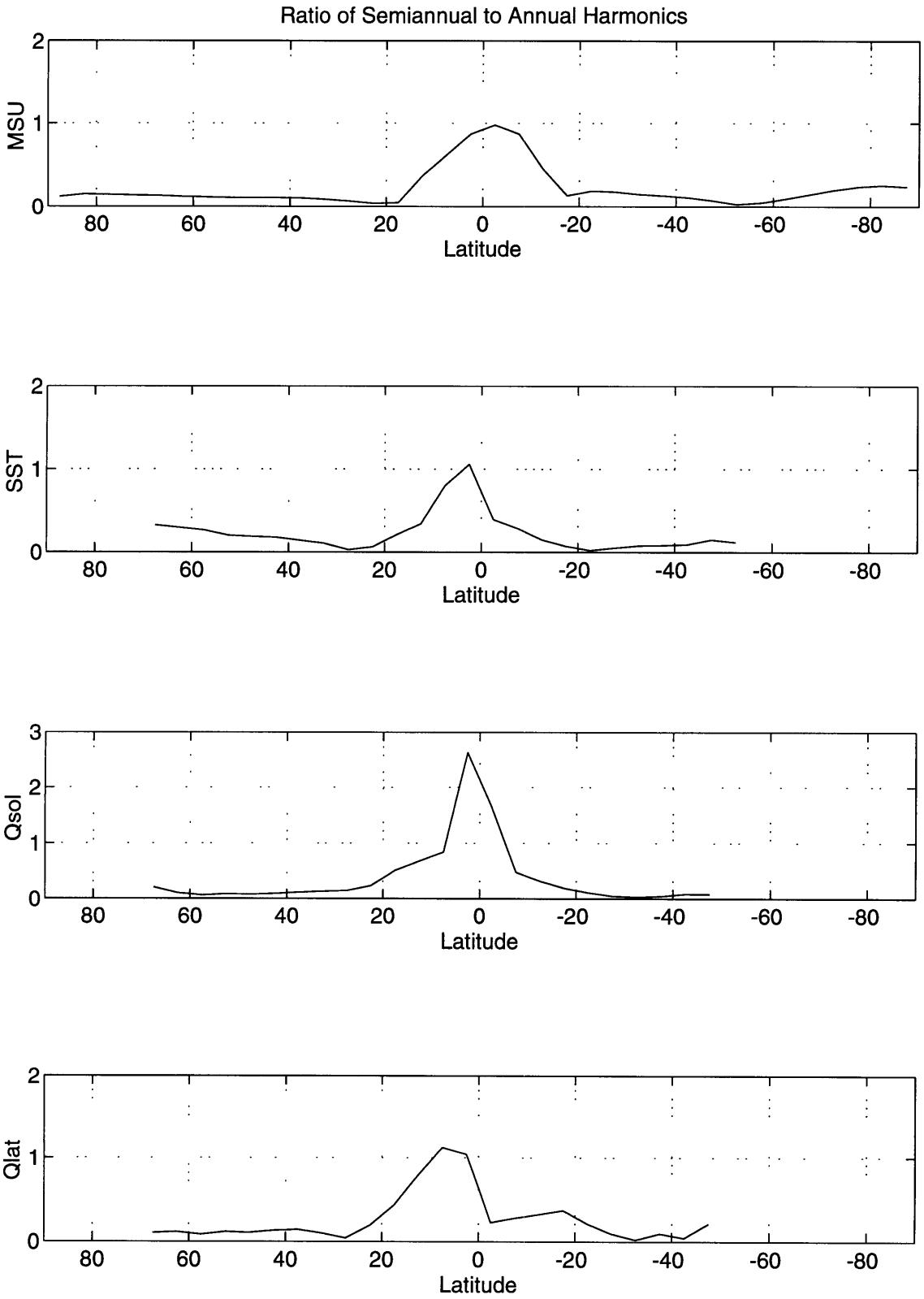

Figure 3-4: Ratios of semiannual to annual amplitudes of zonal averaged MSU, SST, Q_{sol} and Q_{lat}.

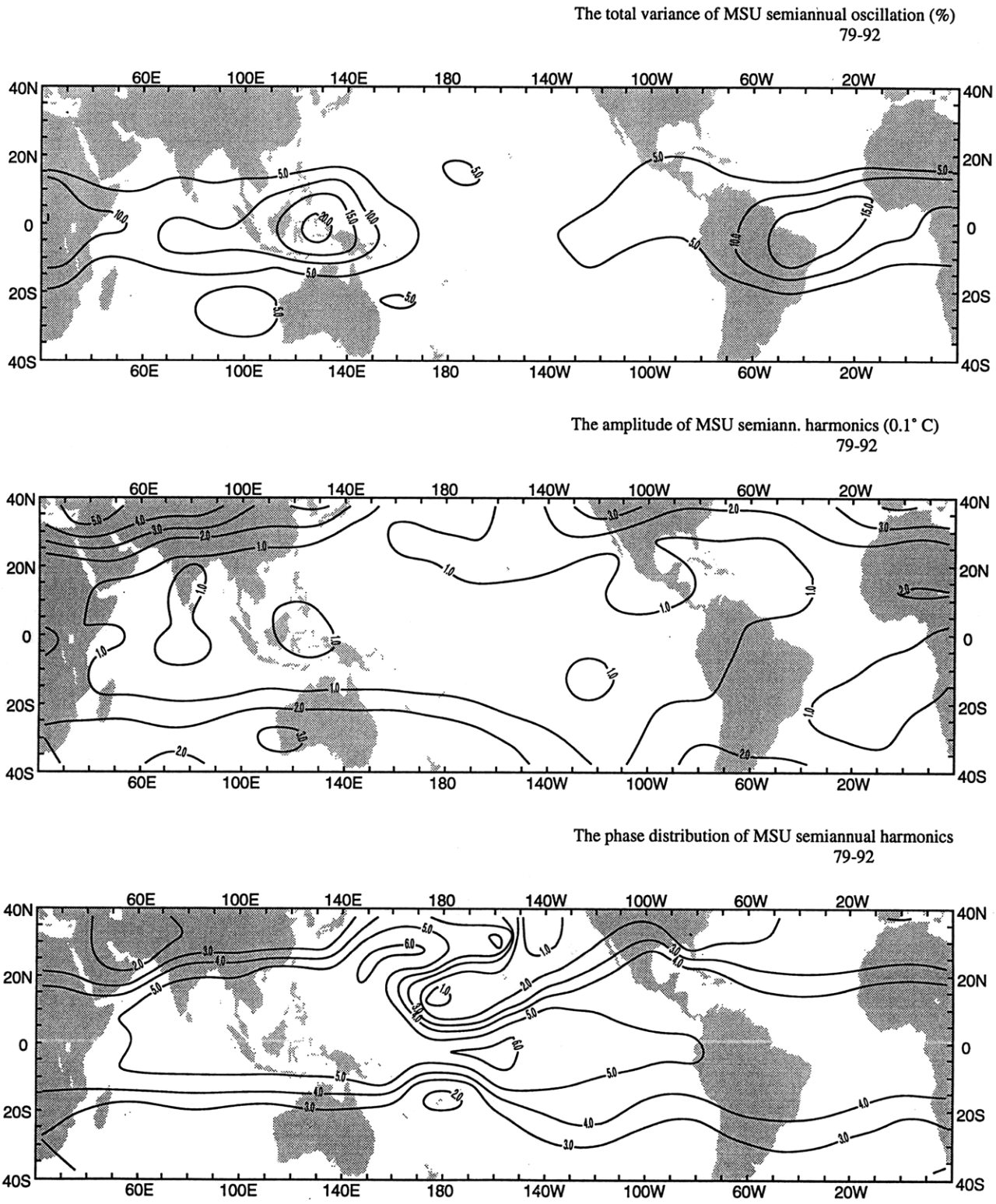

Figure 3-5: (a) The percentage of total variance for MSU semiannual harmonics (40N-40S) during 1979-1992. (b) The amplitude of MSU semiannual harmonics (40N-40S) (c)The phase of MSU semiannual harmonics (40N-40S) during 1979-1992. The phase is marked as 1=January 1; 2=February 1. during 1979-1992.

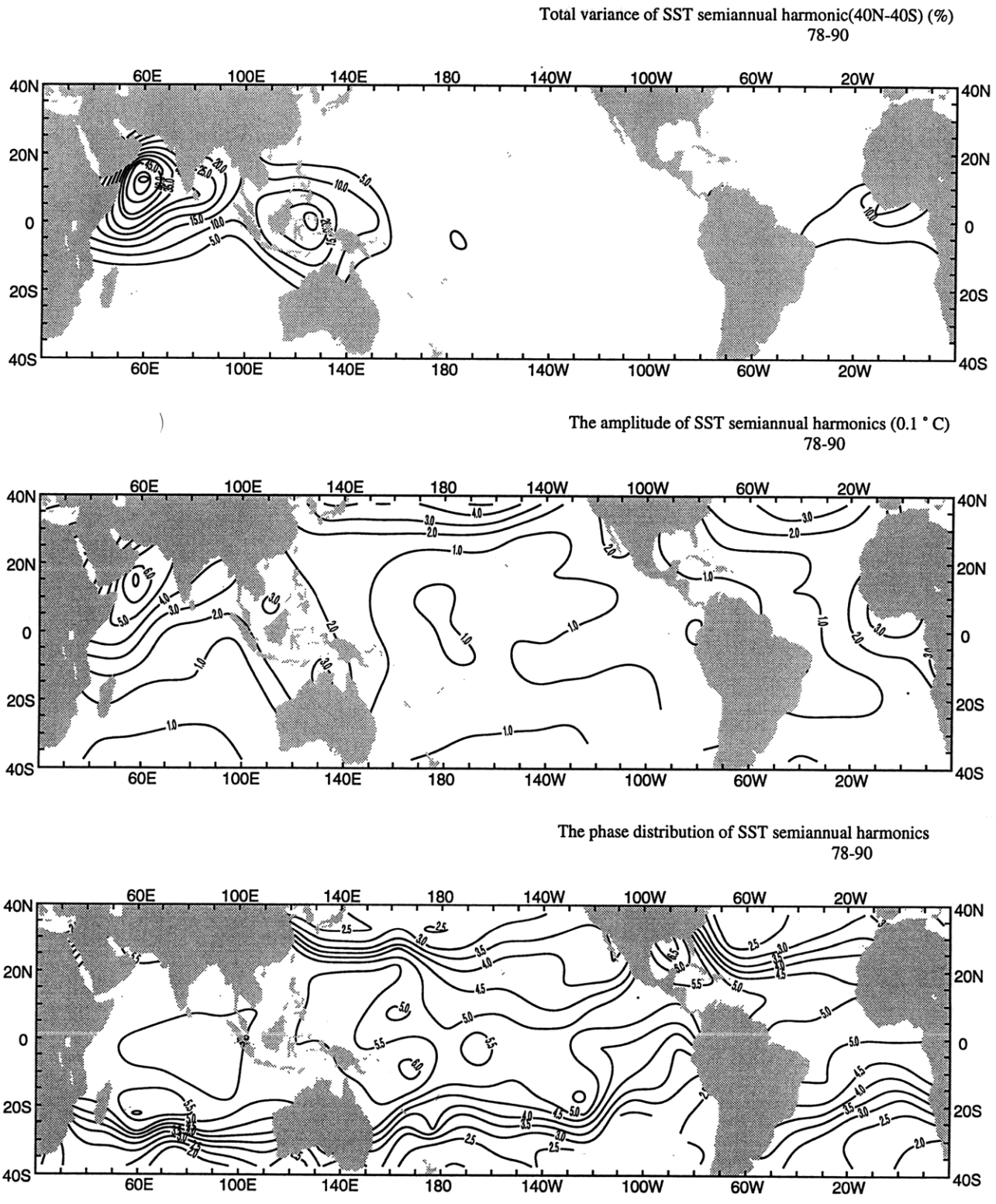

Figure 3-6: (a) Same as Figure 3.5a but for SST during 1978-1990. (b) Same as Figure 3.5b but for SST during 1978-1990. (c) Same as Figure 3.5c but for SST during 1978-1990.

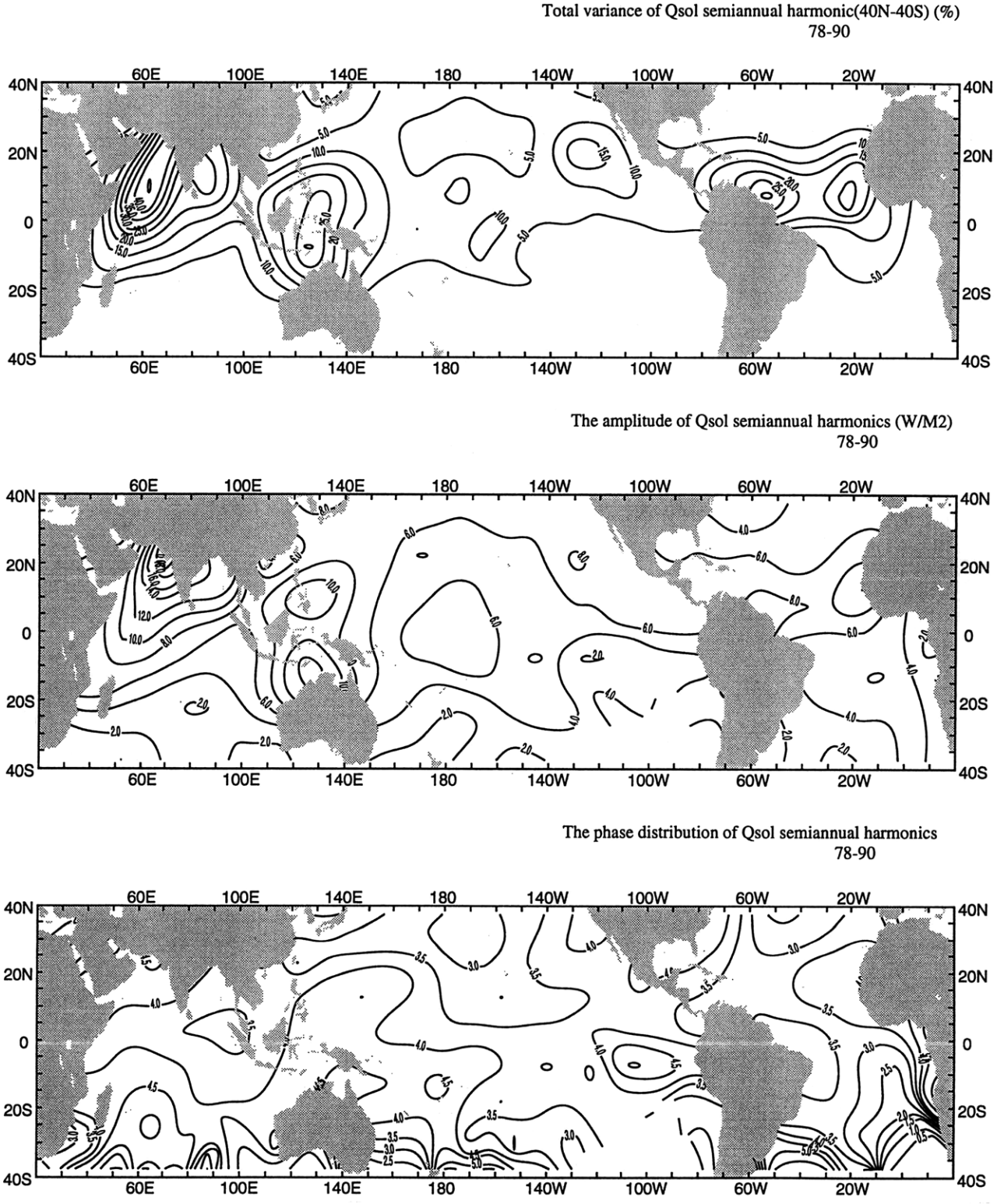

Figure 3-7: (a) Same as Figure 3.5a but for Q_{sol} during 1978-1990. (b)Same as Figure 3.5b but for Q_{sol} during 1978-1990. (c) Same as Figure 3.5c but for Q_{sol} during 1978-1990.

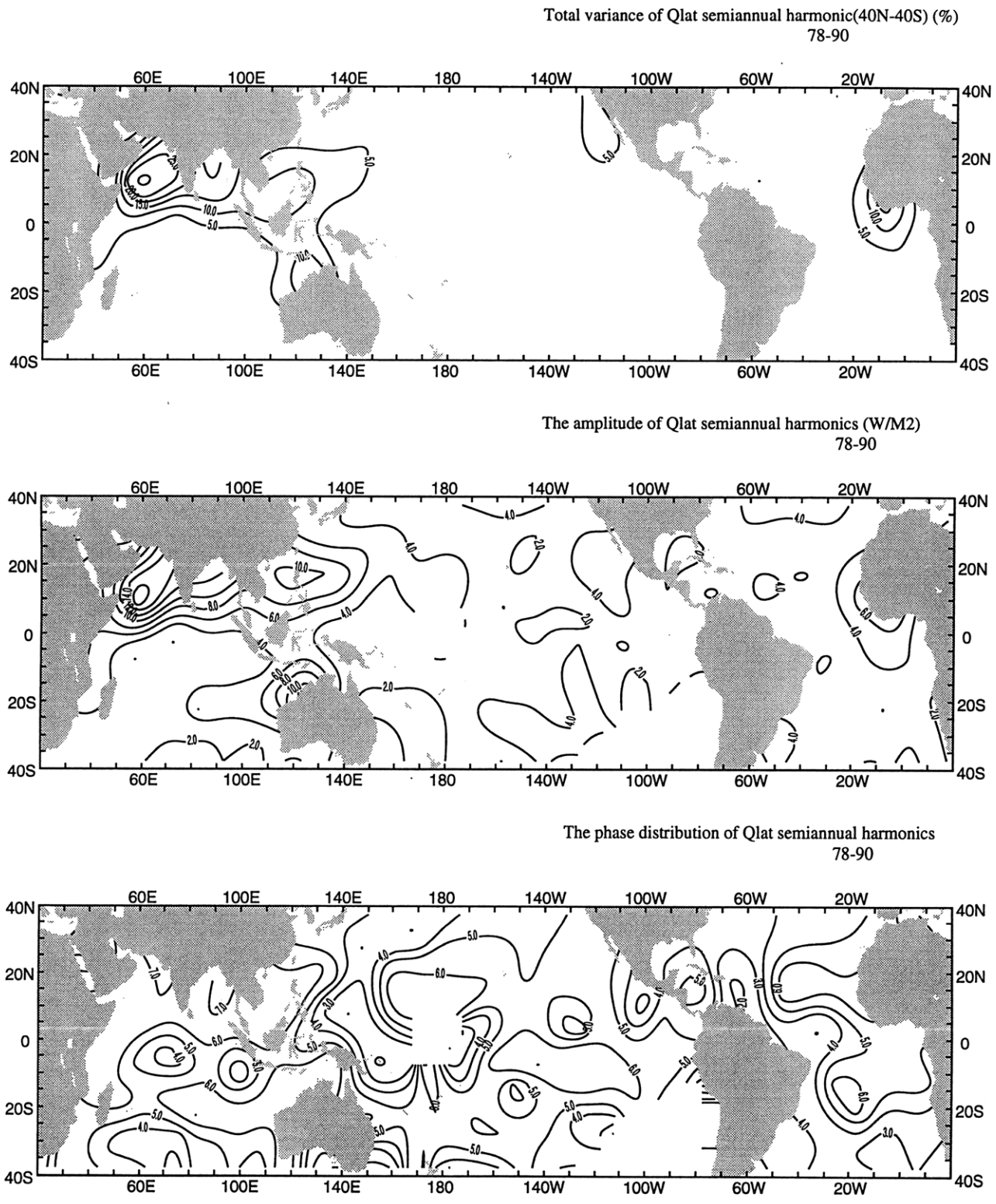

Figure 3-8: (a) Same as Figure 3.5a but for Q_{lat} during 1978-1990. (b) Same as Figure 3.5b but for Q_{lat} during 1978-1990. (c) Same as Figure 3.5c but for Q_{lat} during 1978-1990.

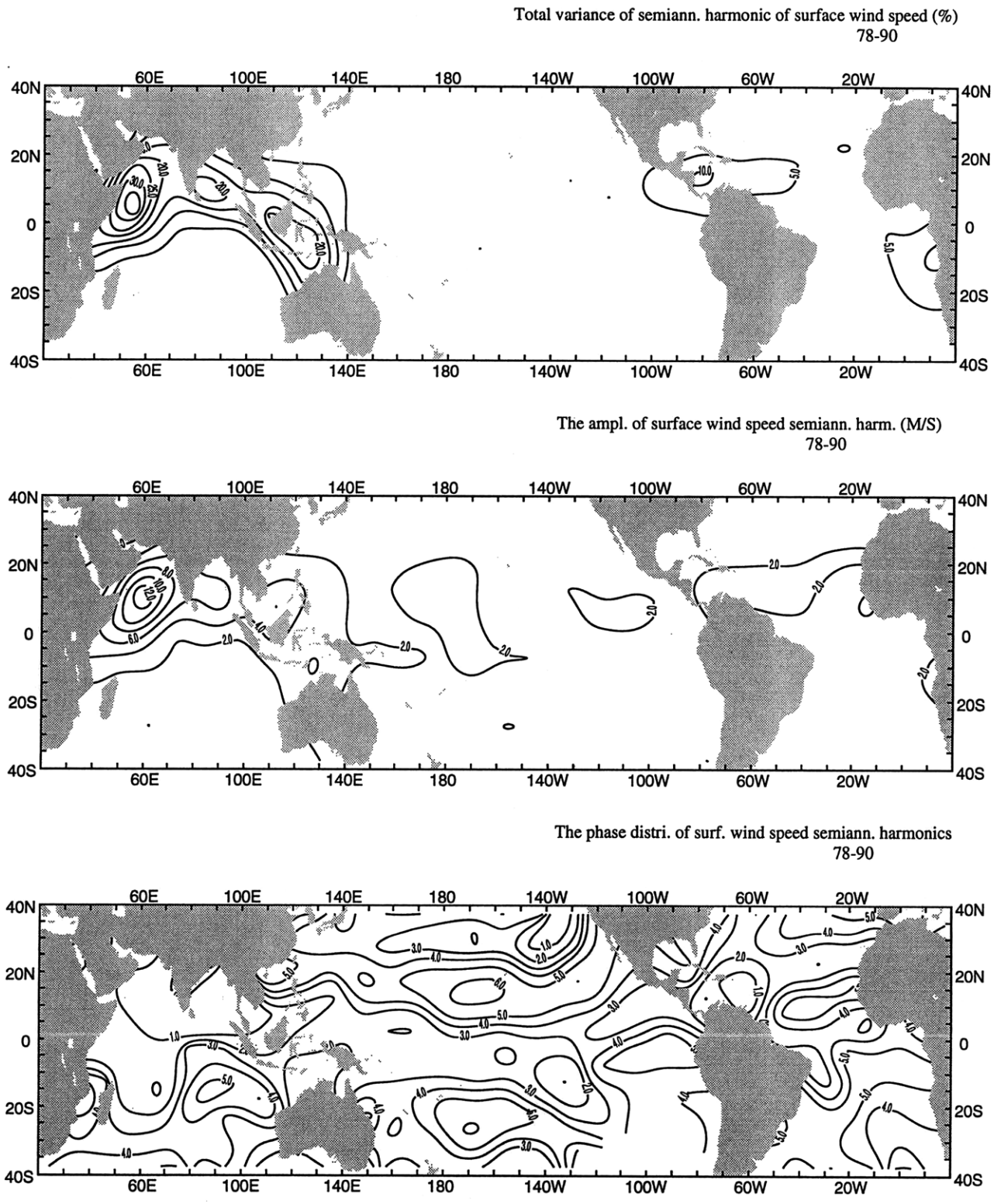

Figure 3-9: (a) Same as Figure 3.5a but for sea surface wind speed during 1978-1990. (b) Same as Figure 3.5b but for sea surface wind speed during 1978-1990.(c) Same as Figure 3.5c but for sea surface wind speed during 1978-1990.

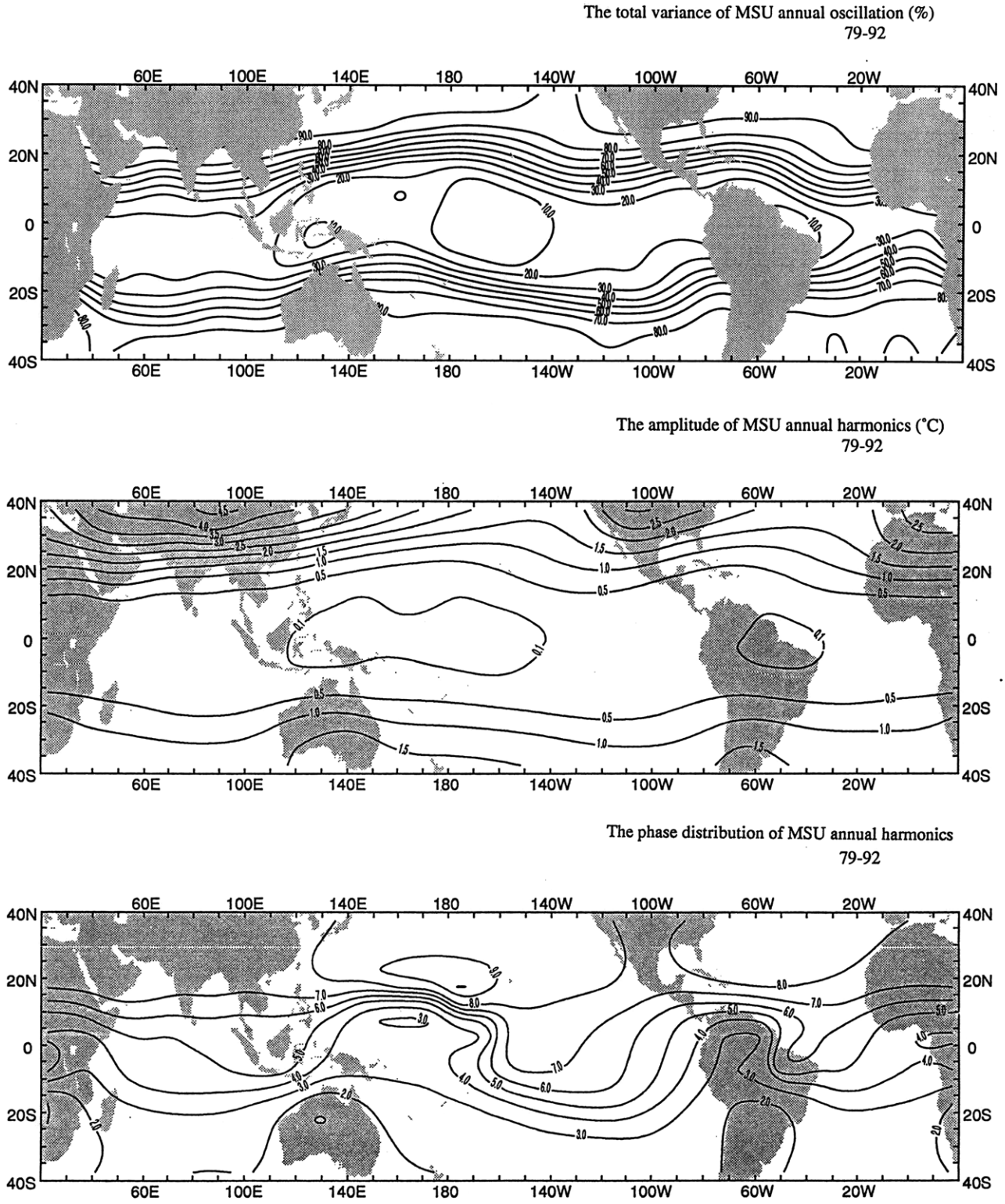

Figure 3-10: (a) The percentage of total variance for MSU annual harmonics (40N-40S) during 1979-1992. (b) The amplitude of MSU annual harmonics (40N-40S). (c)The phase of MSU annual harmonics (40N-40S). The phase is marked as 1=January 1; xsv2=February 1.

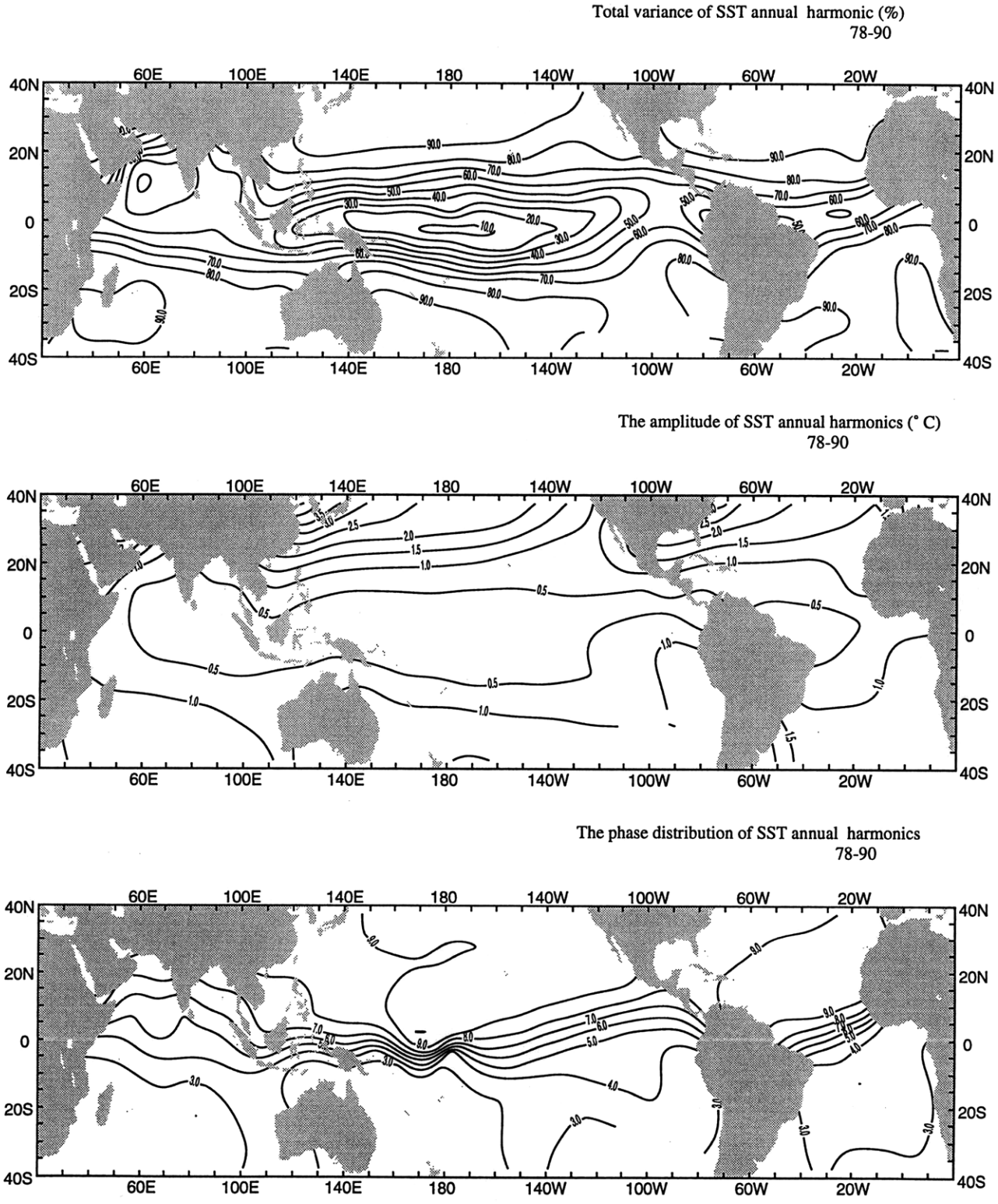

Figure 3-11: (a) Same as 3.10a but for SST during 1978-1990. (b) Same as 3.10b but for SST during 1978-1990. (c) Same as 3.10c but for SST during 1978-1990.

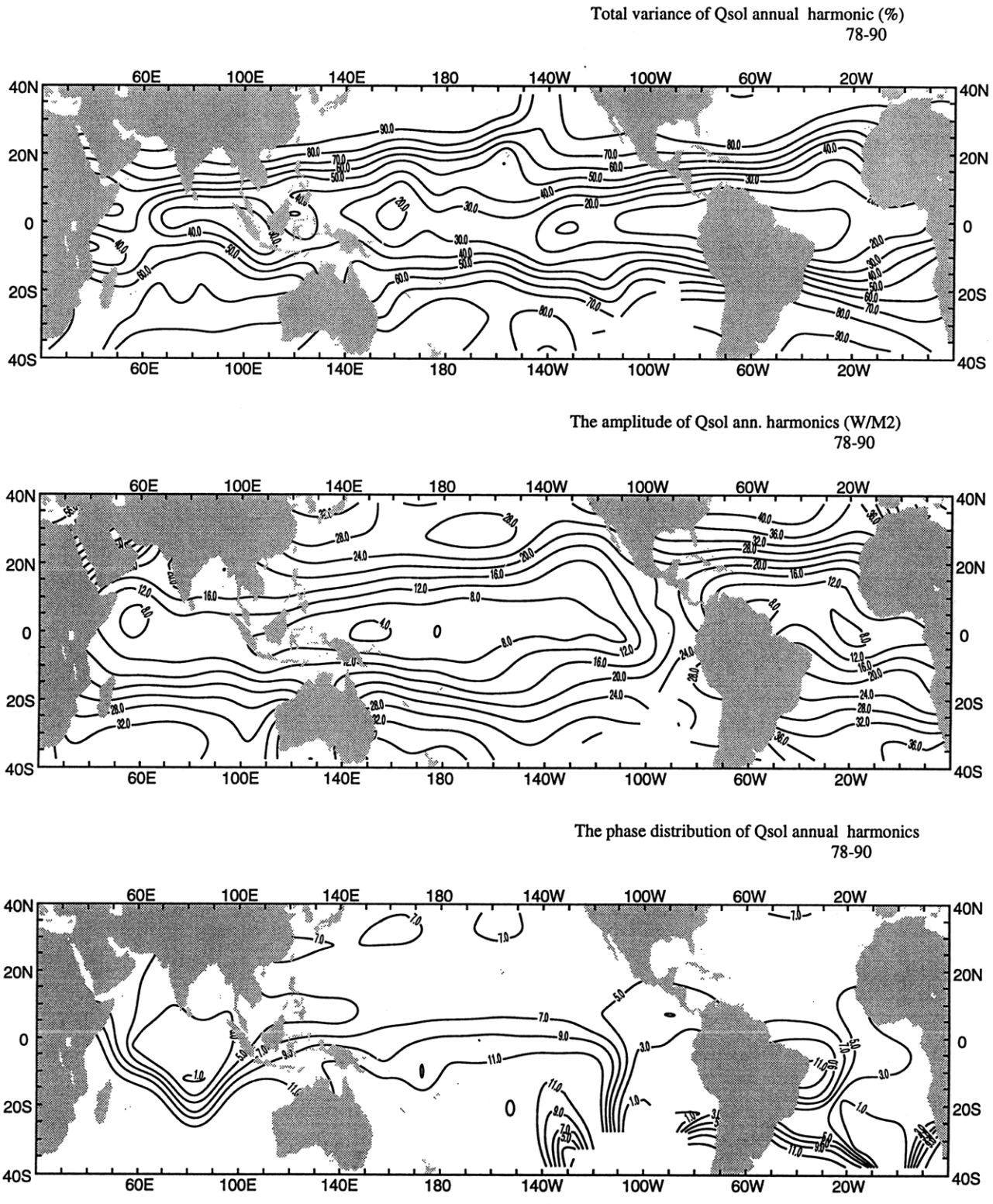

Figure 3-12: (a) Same as 3.10a but for Q_{sol} during 1978-1990. (b) Same as 3.10b but for Q_{sol} during 1978-1990. (c) Same as 3.10c but for Q_{sol} during 1978-1990.

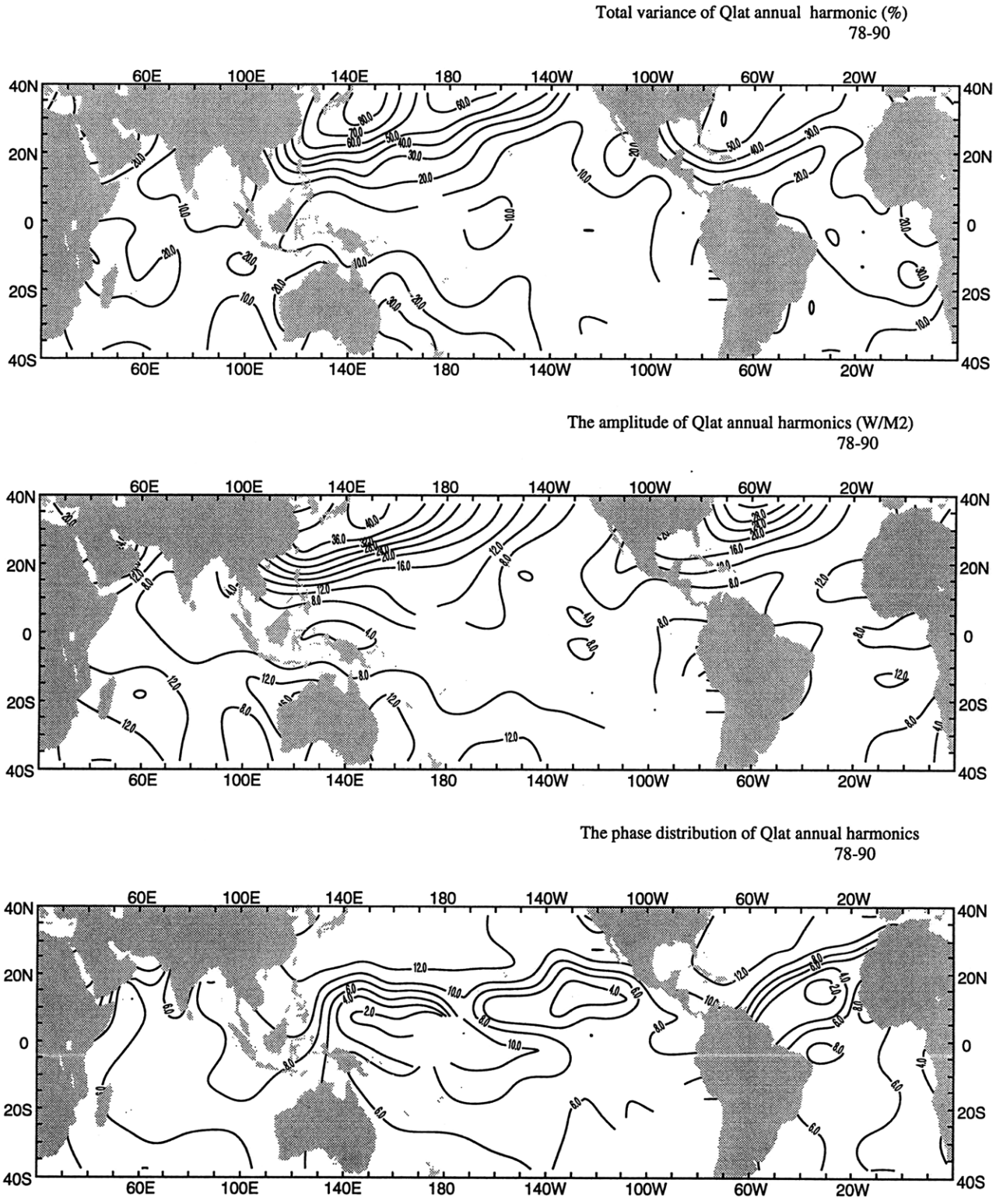

Figure 3-13: (a) Same as 3.10a but for Q_{lat} during 1978-1990. (b) Same as 3.10b but for Q_{lat} during 1978-1990. (c) Same as 3.10c but for Q_{lat} during 1978-1990.

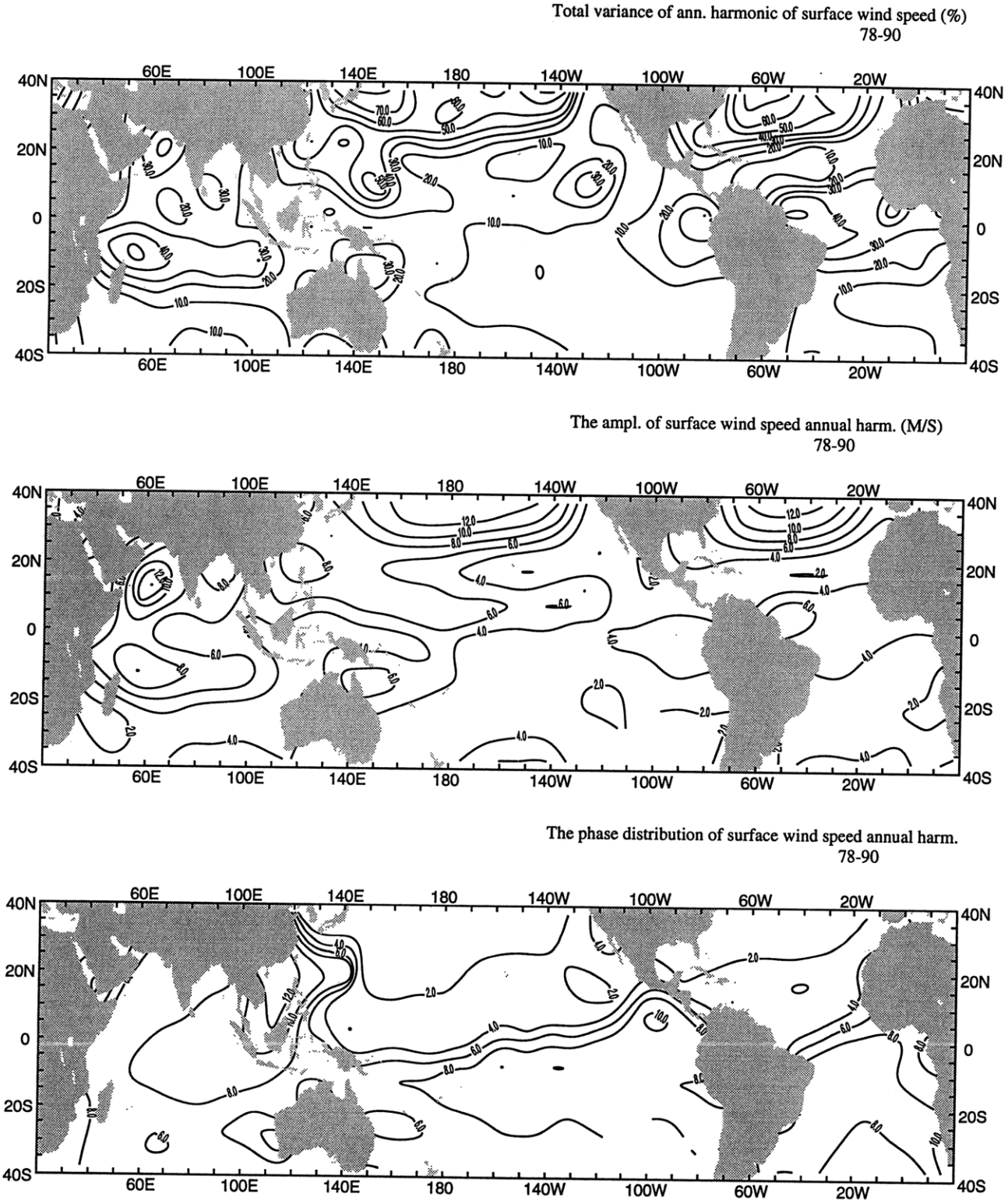

Figure 3-14: (a) Same as 3.10a but for sea surface wind speed during 1978-1990. (b) Same as 3.10b but for sea surface wind speed during 1978-1990. (c)Same as 3.10c but for sea surface wind speed during 1978-1990.

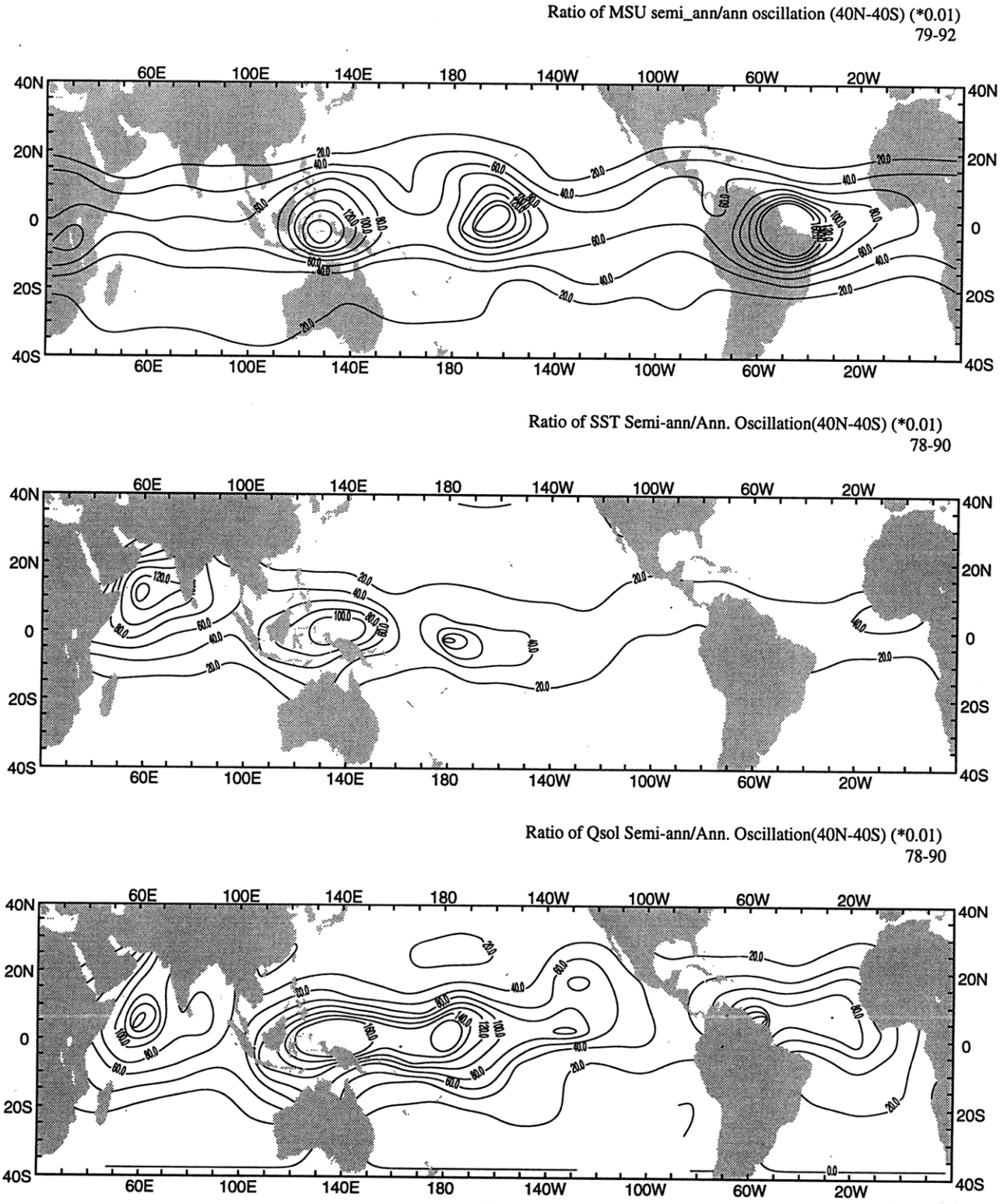

Figure 3-15: (a) Ratio of semiannual to annual amplitudes for MSU (40N-40S). (b) Ratio of semiannual to annual amplitudes for SST (40N-40S). (c) Ratio of semiannual to annual amplitudes for Q_{sol} (40N-40S).

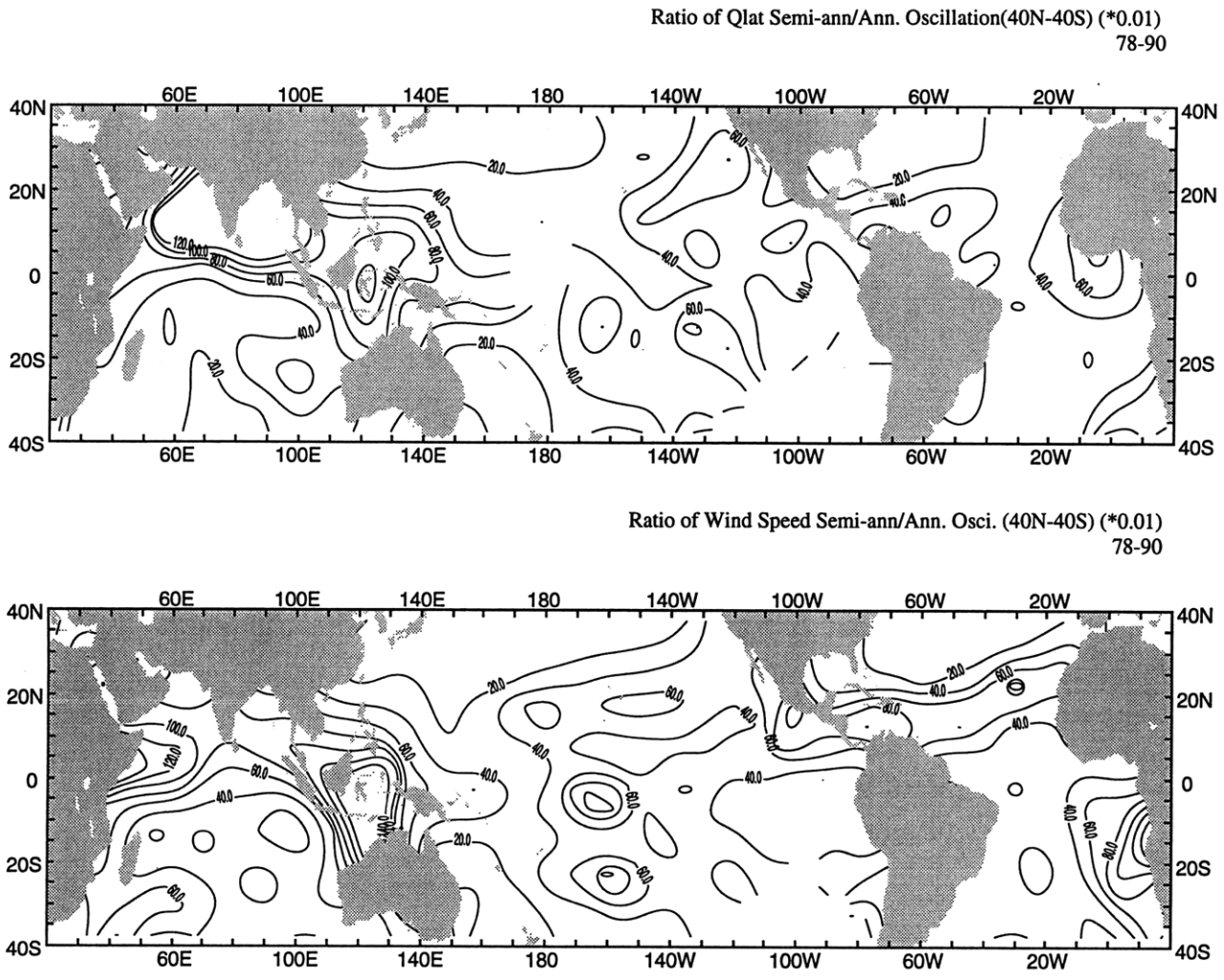

Figure 3-15: (d) Ratio of semiannual to annual amplitudes for Q_{lat} (40N-40S). (e) Ratio of semiannual to annual amplitudes for oceanic surface wind speed (40N-40S).

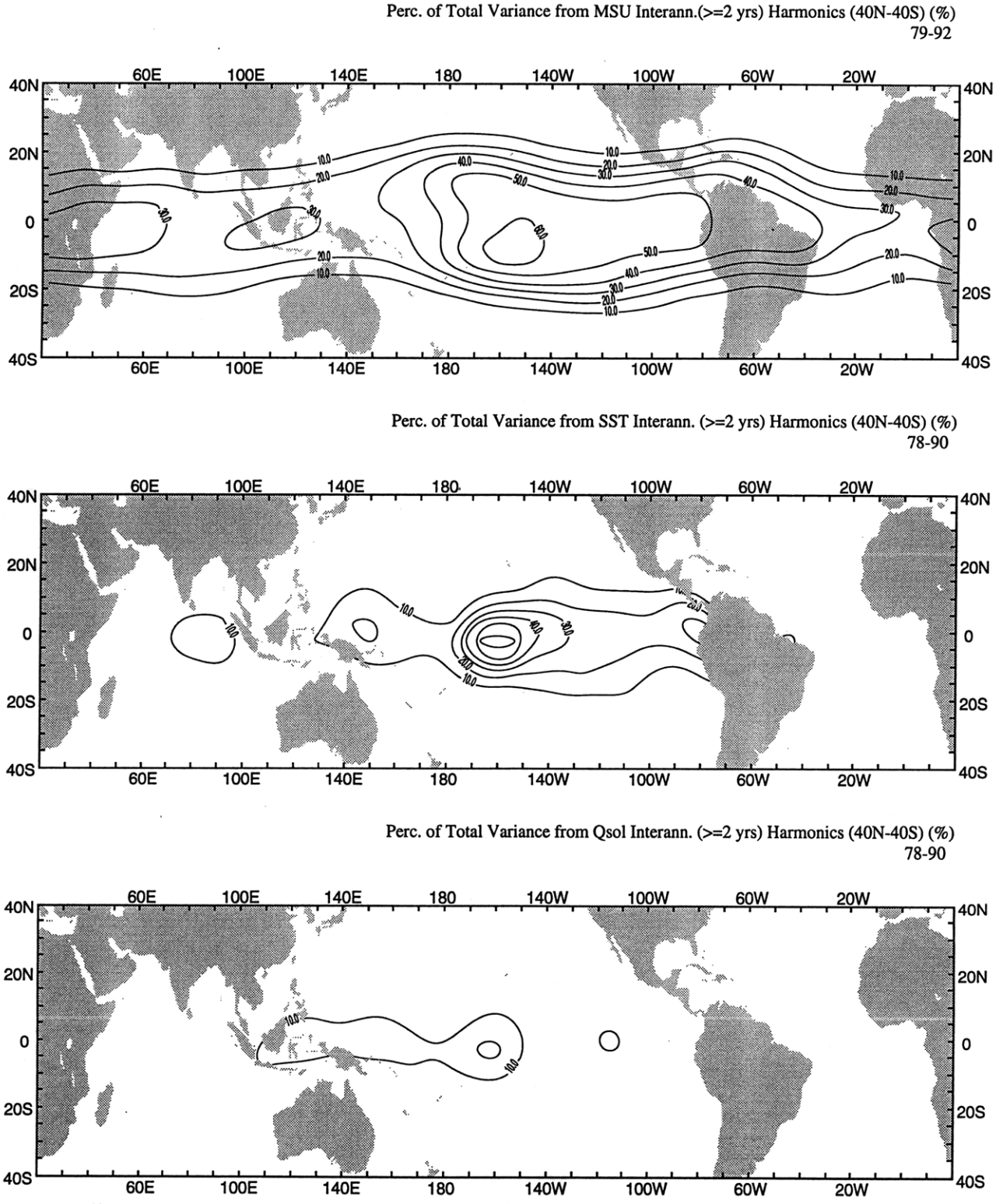

Figure 3-16: (a) Percentage of total variance from MSU interannual (greater than 2 years) harmonics during 1978-1992. (b) Same as 3.16a but for SST during 1978-1990. (c) Same as 3.16a but for Q_{sol} during 1978-1990.

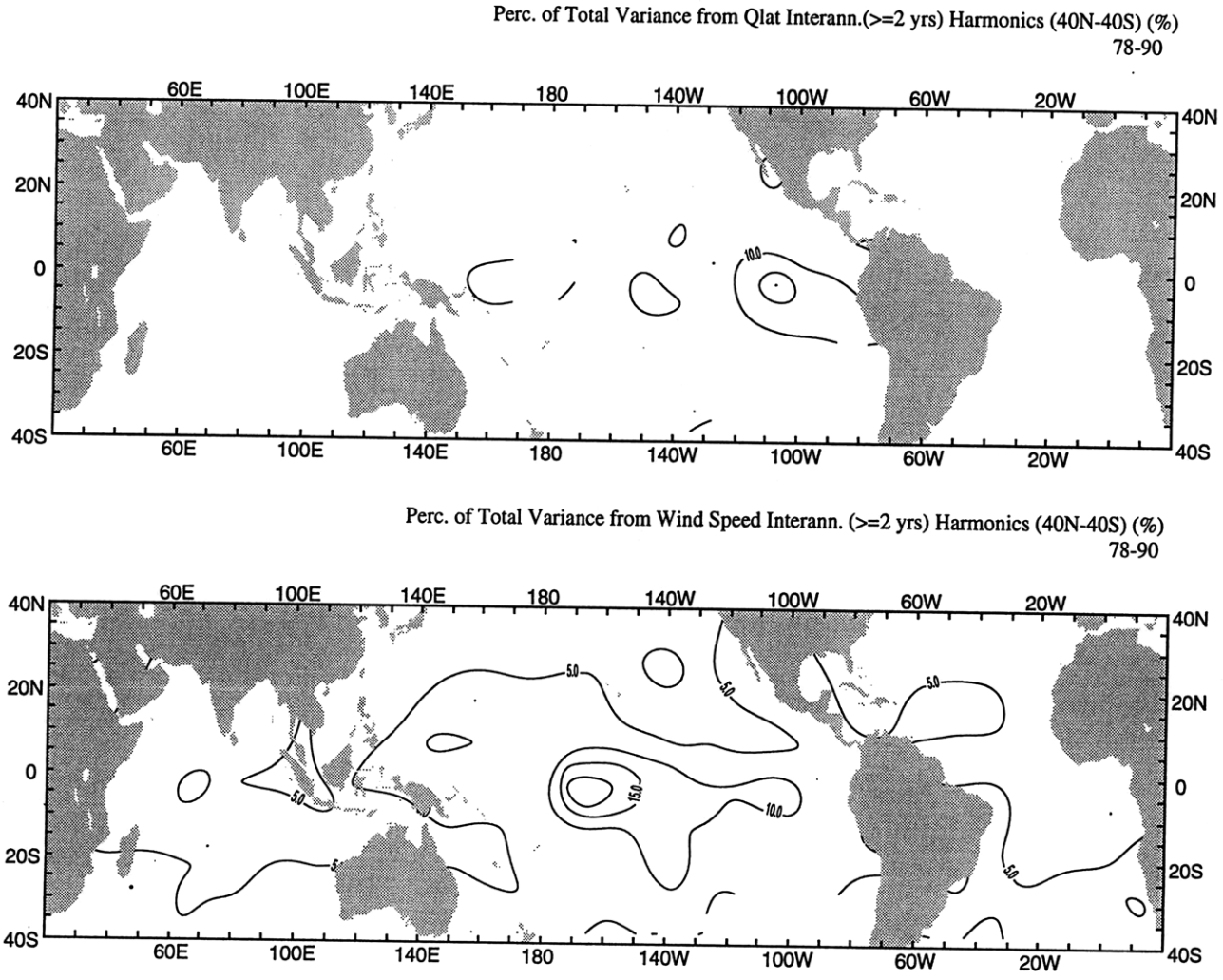

Figure 3-16: (d) Same as 3.16a but for Q_{lat} during 1978-1990.(e) Same as 3.16a but for sea surface wind speed during 1978-1990.

Chapter 4

Discussion of Harmonic Analysis Results

The results of harmonic analysis at different time scales have been presented in the last chapter. We may ask what causes the semiannual oscillations of free air temperature and SST. What are the oceanic effects on the variations of free air temperature? What's the reason for the zonally asymmetric structures in the tropics? In this chapter, the above questions will be discussed. The physical reasons for the semiannual cycle will be stressed.

4.1 Semiannual harmonics

4.1.1 Semiannual harmonics in the tropics

Solar radiation provides the source energy for the climate system. The substantial semiannual radiative forcing in the tropical area(Figure 3.1) (63% of the total variance) indicates the likelihood of a semiannual response in the tropics. From MSU data, the phase of semiannual harmonics of free air temperature (Figure 3.5c) mainly shows the tropical strip pattern with the maximum in May/November. There is an exception in the central northern Pacific area where the phase of the maximum of the semiannual oscillation is January-February (July-August), which stretches from

the North America. But the percentage of total variation of semiannual harmonic is very small in the tropical central Pacific, less than 5%.

What causes the semiannual oscillation of free air temperature? The phase of the maximum of Q_{sol} semiannual oscillation in the tropics (Figure 3.7c) is March/October, which is coherent with the phase of the equinox of solar orbit. But the maximum MSU semiannual cycles occurs in May/November, which is about one or two month lag with the semiannual cycle of tropical solar radiation. It implies that the short-wave and near-infrared heatings by the atmospheric water vapor and CO_2 do not cause the coherent response of the semiannual cycles of free air temperature. How about the indirect heating caused by the atmospheric circulation? Van Loon and Jenne (1970) described the semiannual component for the tropospheric air temperature between 60°E and 120°E. They suggested that the half-yearly variation in the equator is linked with the rising branch of the Hadley circulation which crosses the equator twice a year. With the upward motions of the Hadley cell moving to the equator, the equatorial tropospheric atmosphere is heated by the release of the latent heat. But their results is only a regional feature. The tropical region between 60°E-120°E is an area with intensive cumulus convection related to the Asian and Australian monsoons. In fact, the tropical atmosphere sustains an asymmetric structure for the semiannual mode of the divergence circulation (Chen and Wu, 1992; Weickmann and Chervin 1988), which reveals that a differential response of the atmosphere to the solar heating exists between the land and water dominated hemispheres. Chen and Wu suggested that the land dominated hemisphere ($120°W$-$60°E$) has a quicker response to the equatorial solar heating with the maximum semiannual phase in April/October for outgoing longwave radiation (OLR) and velocity potential while the water dominated hemisphere (60°E-120°W) shows the phase of the maximum of the semiannual cycle for the two components in January/July. In their results, the phase of the maximum of the semiannual modes in the whole tropics is April/October, which is consistent with that in the land dominated hemisphere. But the whole strip of the free air temperature varying at half-yearly cycle acts coherently and there is no difference between the land and water dominated hemispheres. Obviously, it is hard to explain

the tropical symmetric strip structure of free air temperature from the asymmetric divergence circulations in the tropics. In the Asian-Australian monsoon dominated hemisphere(60°E-120°W), the OLR negative anomalies (which shows the positive latent heat release in the atmosphere) appear in January/July for the semiannual cycle, while free air temperature in the same region doesn't show the positive peaks at the same time.

What causes free air temperature varying coherently in the whole tropical zone with the maximum phase in May/November? SST shows its maximum semiannual phase in May/November everywhere (Figure 3.6c). In the mode paper, the authors pointed out the similarity between semiannual Q_{sol} and SST patterns and suggested that Q_{sol} could be the driving force on the semiannual variances of SST. SST is about two months lagged on Q_{sol} in the tropics. The semiannual SST variation at the surface could be the forcing for the semiannual cycles of free air temperature. But from the Q_{lat} data used in the current paper, the data shows some patchy structure. The first maximum for semiannual Q_{lat} varies from April to June in the tropics (Figure 3.8c). There is no consistent phase patterns.

4.1.2 MSU semiannual harmonics in the middle and high latitudes

The total variance of MSU semiannual harmonics represents a small part of total variation in the middle and higher latitudes, where the annual oscillations are dominant. The zonal averaged MSU value shows that the phase of semiannual harmonic in the southern hemisphere changes gradually (30S-70S) from May/November in the tropics to July/January in the higher latitudes (Figure 3.3). But in the NH, the phase of the maximum changes more abruptly around 20N between the one in tropics(0-20N) (May/November) and the one in the middle and high latitudes(30N-90N) (January/July). Van Loon and Jenne(1970) proposed the air temperature semiannual cycle could be related to the jet stream, which is associated with the poleward arm of the Hadley circulation. According to the thermal wind relationship, tropospheric up-

per level wind could be closely related to the free air temperature variations. Future work needs to be done on the variations of the tropospheric upper level wind. Currently, it is hard to give reasonable physical answers on the phase difference between NH and SH.

Compared with the zonally symmetric structure of MSU semiannual harmonics, the patterns of the semiannual harmonics of SST and surface heat flux are rather asymmetric. In the Indian monsoon region and tropical west Pacific, the percentage of total variance contributed by the semiannual oscillations are relatively larger than the ones in the other region. From the phase differences among Q_{lat}, SST and oceanic surface wind speed(Figure 3.6c, 3.8c and 3.9c), it seems that the variations of semiannual Q_{lat} are not only dependent upon the change of SST or oceanic surface wind speed. The combined effects from SST and oceanic surface wind effects, as well as the variations of atmospheric humid fields at the ocean surface, should be considered to estimate the Q_{lat} change.

4.2 Annual and interannual harmonics

In the tropics, the percenatge of total variance of the annual harmonic reaches the minimum. The phases of annual harmonics are in the transition seasons(spring or autumn) for MSU and SST. The percentage of total variance and phase of the maximum of annual MSU and SST are both longitudinally asymmetric. In the remote equatorial central Pacific the annual oscillations for both SST and MSU have the smallest values. The phase distribution of SST annual maximum skews northeastward in the equatorial central and eastern Pacific and equatorial Atlantic. The phase of Q_{sol} annual maximum shows the phase difference in the eastern side of Pacific and Atlantic, where it is least cloudy in May or March. In the current analysis, the patterns of total contribution and amplitudes of annual harmonics between SST and Q_{sol} are close to each other. In the analysis of EOF results (Hu, Newell and Wu 1994), the annual patterns between SST and Q_{sol} are also similar. It was proposed that the asymmetric pattern of SST may be mainly caused by the asymmetrics of Q_{sol}. But the phase

distribution in the eastern Pacific and Atlantic seems to suggest the less correlation between SST and Q_{sol} in these areas, where upwelling is a dominant factor on SST in the eastern ocean.

Tropical strip pattern for MSU interannual harmonics is shown clearly in the maps of its total variance (Figure 3.16a). It is mainly associated with the SST ENSO pattern in the tropical central and eastern Pacific. Comparing with the total variance of MSU and SST, the contributions from the interannual Q_{lat} and Q_{sol} are relatively small. For Q_{lat}, the total variance greater than 10% is situated in the equatorial eastern Pacific (Figure 3.16d). But the evaporation released from this area is responsible for the atmospheric heating in the entire tropical strip(Hu, Newell and Wu 1994). The 10% contour from the total variance of Q_{sol} interannual harmonic is mainly in the western and central Pacific, which is not as clear as the nonseasonal Q_{sol} EOF results which indicates the enhancement of convection in the equatorial central Pacific.

Chapter 5

Concluding Remarks and Future Works

5.1 Concluding remarks

The main results from the the harmonic analysis and discussion are summarized in the following:

- The zonal mean semiannual harmonics have a large percentage of the total variance in the tropics. The zonal mean Q_{sol} shows that the semiannual harmonic represents 64% of total variance near the equator. SST semiannual harmonic has about 20% of total variance. And the semiannual harmonic of MSU contributes 12% of total variance in the tropics. For Q_{lat}, the semiannual variance has only 10% of total variance.

  The phase of the semiannual harmonic for each component varies in the tropics. The maximum phases for SST and MSU are mainly in May/November while Q_{sol} shows its maximum in March/September. The phase difference between Q_{sol} and MSU suggests no coherent response in the atmospheric free air temperature caused by the direct solar radiation. The large heat capacity in the ocean could be the explanation for the semiannual SST cycles being two months lagged on the direct solar radiative forcing. It is proposed that SST forcing could be the

reason for the semiannual cycles of free air temperature in the whole tropical strip.

The semiannual oscillation becomes less important in the total variance in the middle and high latitudes where the annual cycles are dominant. The phase of semiannual oscillations for free air temperature and SST changes to winter and summer time, which causes the maximum temperature in the summer to be sharper than the minimum in the winter (White and Wallace, 1978).

- Annual harmonics also show equatorial and longitudial asymmetries. In the tropical western and central Pacific, and equatorial eastern Pacific, the MSU annual variations has a small value (less than 10%). For SST, the total variance of the annual harmonics can also reach less than 10% in the tropical central Pacific.

- ENSO signals have a large effect on the tropical MSU. The total percentage of MSU interannual variations in the tropics is about 30% in the tropical west Pacific to 60% in the tropical central and east Pacific. For SST, Q_{lat} and Q_{lat}, the large interannual variations mainly occur in the tropical central and east Pacific, which are associated with ENSO phenomena.

5.2 Future works

Although the SST semiannual cycles at the surface boundary is proposed to be the cause for MSU semiannual oscillations in the tropics, future studies need to be done to show why it is hard to see the direct linkage with the oceanic surface latent flux. The interaction between air and sea has been mainly discussed at the annual and interannual time scales. The physical picture is still not clear at the semiannual modes.

Zonally asymmetric structures are shown clearly in the harmonics results of the tropical data though the solar radiation at the top of the atmosphere is totally zonal symmetric. Even MSU data shows a tropical strip structure in the different kinds of

harmonics, but its amplitude still varies zonally. What causes the equatorial asymmetries? Is it due to the difference between land and sea at the tropical surface or even caused by the different eddies forcing between NH and SH?

References

Barnett, T.P., M. Latif, E. Krik and E. Roeckner, 1991: On ENSO Physics J. Climate, **4**, 487-515.

Bjerknes, J.,1969: Atmospheric teleconnections from the equatorial Pacific. Mon. Wea. Rev., **97**, 163-172.

Bunker, A.F., 1976: Computations of surface energy flux and annual air-sea interaction cycles of the North Atlantic Ocean. Mon. Wea. Rev., **104**, 1122-1140.

Budyko, M.I. 1963: Atlas of the heat balance of the Earth. Gidrometeorozdat, Moscow.

Chen T-C, and K-D Wu, 1992: Semi-annual oscillation of the global divergent circulation. Tellus, **44A**, 357-365.

Cornejo-Garrido, A.G. and P.H., Stone, 1977: On the heat balance of the Walker Circulation. J. Atmos. Sci., **34**, 1155-1162.

Cayan, D.R. 1992: Latent and sensible heat flux anomalies over the northern oceans: driving the sea surface temperature. J. Phys. Oceanogr., **22**, 859-881.

Deser C. and J.M. Wallace 1990: Large scale atmospheric circulation features of warm and cold episodes in the tropical Pacific. J. Climate, **3**, 1254-1281.

Fu, R., A. D. Del Genio, W. B. Rossow and W. T. Liu, 1992: Cirrus-cloud thermostat for tropical sea surface temperatures tested using satellite data. Nature, **358**, 394-397

Gill, A. E. 1980: Some simple solution for heat-induced tropical circulations. Q. J. R. Met. Soc., **106**, 447-462.

Horel, J.D. and J.M. Wallace, 1981: Planetary-scale atmospheric phenomena associated with the Southern Oscillation. Mon. Wea. Rev., **109**, 813-829.

Hsiung, J., 1986: Mean Surface Energy Fluxes over the Global Ocean. J. Geophys. Res., **91**, 10,585-10,606.

Hsu, C-P. F., and J.M. Wallace, 1976a: The global distribution of the annual and semiannual cycles in precipitation. Mon. Wae. Rev., **104**, 1093-1101.

Hsu, C-P. F., and J.M. Wallace, 1976b: The global distribution of the annual and semiannual cycles in sea level pressure. Mon. Wea. Rev., **110**, 1335-1346.

Hu, W., R. E. Newell and Z. Wu 1994: Modes of variability of global sea surface temperature free air temperature and oceanic surface energy flux. Climate Dynamics, **10**, 377-393.

Jenkins, G.M. and D.G. Watts 1968: Spectral analysis and its applications. Holden-Day, Inc. pp525.

Large W. and S. Pond, 1992: Sensible and latent heat flux measurements over the ocean. J. Phys. Oceanogr., **12**, 464-482.

Lau, N.C. 1985 : Modeling the seasonal dependence of the atmospheric responses to observed El Niños 1962-1976. Mon. Wea. Rev., **113**,1970-1996.

Lindzen, R.S., and S. Nigam, 1987: On the role of sea surface temperature gradients in forcing low level winds and convergence in the tropics. J. Atmos. Sci., **44**, 2418-2435.

Meehl, G.A. 1987: The annual cycle and interannual variability in the tropical Pacific and Indian Ocean regions. Mon. Wea. Rev., **115**, 27-50.

Newell, R.E. and Z. Wu, 1992: The interrelationship between temperature changes in the free atmosphere and sea surface temperature changes. J. Geophys. Res., **97**, 3693-3709.

Pan, Y.H. and A.H. Oort, 1983: Global climate variations connected with sea surface temperature anomalies in the eastern equatorial Pacific ocean for the 1953-73 period. Mon. Wea. Rev., **111**, 1244-1258.

Ramanathan, V., R. D. Ross, E. F. Harrison, P. Minnis, B. R. Barkstrom, E. Ahmad and D. Hartmann, 1989: Cloud-radiative forcing and climate: results from the Earth Radiation Budget Experiment. Science, **243**, 57-63.

Ramanathan, V., and W. Collins, 1991: Thermodynamic regulation of ccean warming by cirrus clouds deduced from observations of the 1987 El Niño. Nature, **351**, 27-32.

Rasmusson, E.N., and T.H. Carpenter, 1982: Variations in tropical sea surface temperature and surface wind fields associated with the Southern Oscillation/ El Niño. Mon. Wea. Rev.,**110**, 354-384.

Spencer, R.W., J.R. Christy and N.C. Grody, 1990: Global atmospheric tempera-

ture monitoring with satellite microwave measurements: methods and results 1979-84. J. Clim., **3**, 1111-1128.

Wallace, J.M., 1992: Effect of deep convection on the regulation of tropical Sea Surface Temperature. Nature, **357**, 230-231.

Wang Bin, 1994: Climatic regimes of tropical convection and rainfall. J. Climate, **7**, 1109-1118.

Weare, B.C. and P.T. Strub, and M.D. Sauel, 1981: Annual mean surface flux in the tropical ocean, J. Phys. Oceanogr., **11**, 705-717.

Webster, P.J. 1972: Response of the Tropical Atmosphere to Local Steady Forcing. Mon. Wea. Rev.,**100**, 518-541.

Webster, P.J. 1982: Seasonality in the local and remote atmosphere response to sea surface temperature anomalies. J. Atmos. Sci.,**39**, 41-52.

Weickmann, K.M. and R.M. Chervin, 1988: The observed and simulated atmospheric seasonal cycle. Part I: Global wind field modes. J. Climate, **1**, 265-290.

White, G. H. and J.M. Wallace, 1978: The global distribution of the annual and semiannual cycles in surface temperature. Mon. Wea. Rev., **106**, 901-906.

Van Loon, H. and R. L. Jenne, 1969: The half yearly oscillations in the tropics of the Southern Hemisphere. J. Atmos. Sci., **26**, 218-232.

Van Loon, H. and R. L. Jenne, 1970: On the half-yearly oscillations in the tropics. Tellus, **22**, 391-398.